

A Model of Bank Failures: Funding Frictions and the Dynamics Before Collapse*

João Pedro Rudge Leite †

University of Arkansas

November 27, 2025

[[Click here for latest version](#)]

Abstract

This paper develops a quantitative model of bank failures to examine how funding frictions shape balance-sheet pressures and the timing of default. Banks in the model face limited commitment, capital regulation, and costly access to illiquid liabilities. By issuing both deposits and time deposits, they manage short-run liquidity needs but increase their future repayment obligations and exposure to default. Default arises endogenously when equity falls below regulatory thresholds. The model shows that liability composition is a central determinant of banks' resilience: long-term funding mitigates rollover risk and supports smoother cash flows in normal times, but heightens vulnerability once profitability and asset quality deteriorate. This dual role of time deposits generates the gradual rise in leverage, tightening margins, and accelerating credit losses that precede failure. The analysis demonstrates that funding structure is a key driver of bank stability and of the dynamics that push distressed institutions toward default.

*I am grateful to Yan Bai for her guidance and support. This project benefited from numerous conversations with George Alessandria and Matias Moretti.

†Department of Economics, University of Arkansas. E-mail jrudgeleite@walton.uark.edu

1. Introduction

Banks do not fail overnight. Years before default, they display a consistent pattern: leverage drifts upward, net interest margins compress, and the share of time deposits steadily increases. These patterns suggest that the liability side of the balance sheet plays an active role in shaping a bank’s deterioration, rather than simply reflecting underlying distress. This paper develops a model that explains these dynamics and quantifies the mechanisms that move banks from stability toward failure.

The central premise is that banks’ funding structures can be stabilizing in some environments and destabilizing in others. Short-term deposits provide flexibility but must be rolled over frequently, while long-term deposits, such as time deposits, offer more stable funding at the cost of future repayment obligations. In normal conditions, time deposits help smooth liquidity needs and reduce rollover pressure. But when profitability deteriorates and credit losses rise, the same illiquidity tightens balance-sheet constraints and accelerates the transition toward default. Understanding this dual role of funding instruments is essential for explaining why distress emerges gradually and why failures occur when they do.

To formalize this mechanism, I develop a dynamic model in which heterogeneous banks choose between deposits and time deposits while facing liquidity shocks, limited commitment, and capital requirements. Time deposits reduce rollover risk but increase future interest expenses and repayment obligations. Default arises endogenously when equity falls below regulatory thresholds, generating a stationary distribution of banks across solvency states. The resulting dynamics mirror those observed in empirical event studies of failed institutions: rising leverage, increased reliance on time deposits, compressing net interest margins, and escalating charge-offs.

A key contribution of the paper is to quantify the forces that lead banks toward default. Using a variance decomposition of expected default over event time, I assess how three state variables—funding composition, leverage, and credit losses—explain cross-sectional differences in default risk. Three findings emerge. First, credit losses are the dominant driver of default risk in the periods immediately preceding failure, reflecting the sharp deterioration in asset quality near the end of the bank’s life cycle. Second, funding composition—particularly the share of time deposits—matters throughout the buildup to distress. Early on, time de-

posits stabilize funding; later, their illiquidity increases repayment pressure exactly when earnings weaken. Third, leverage explains relatively little of the variation in expected default, becoming important only when the bank is already close to failing. These patterns reveal that the transition to default is driven by evolving interactions between earnings, funding choices, and liquidity stress—not by static balance-sheet ratios alone.

These results clarify why time deposits become increasingly important as banks approach distress. Early in the cycle, they allow banks to avoid forced deleveraging by smoothing liquidity needs. But as fundamentals deteriorate and repayment obligations loom, banks lose the ability to absorb further shocks. The same funding that once stabilized the balance sheet begins to amplify distress, generating a gradual but accelerating path to default that does not arise in models with exogenous failure or without funding frictions.

The model also offers a tractable environment for evaluating regulation. Raising the Tier 1 capital requirement to 8 percent reduces failure risk not by shifting average leverage — banks already hold internal buffers — but by lowering the probability of entering states where liquidity stress and credit losses reinforce each other. This improvement in stability occurs with minimal impact on lending or balance-sheet scale.

Taken together, the analysis demonstrates how funding structure and regulatory constraints jointly shape resilience and the timing of bank failures. Time deposits protect banks in normal conditions, but increase vulnerability once fundamentals weaken. Higher capital requirements reduce the likelihood that banks reach states where these pressures become mutually reinforcing. The paper’s central message is that understanding bank failure requires understanding the dynamic interaction of earnings, liquidity, and the maturity structure of bank liabilities.

Related Literature

This paper contributes to several strands of research on bank fragility, funding structure, and financial frictions.

First, it connects to the empirical literature on bank failures and funding composition. Recent work has documented that deteriorating banks experience a progressive shift in their liabilities toward costlier and less stable sources of funding (Correia et al., 2023; Chen et al.,

2024). This paper complements these findings by providing a rationale for the joint evolution of leverage, funding structure, and profitability in the years preceding default. In contrast to existing studies that focus primarily on depositor behavior or run dynamics, I emphasize how banks' own funding choices—particularly the reliance on time deposits—shape their resilience to shocks and the timing of default.

Second, it contributes to the theoretical and quantitative literature on financial frictions and default risk. Building on the tradition of limited-commitment models (e.g., Arellano et al., 2019; Ottonello and Winberry, 2020; Amador and Bianchi, 2024), the model developed here features banks that issue both short- and long-term liabilities under regulatory and liquidity constraints. As in Gertler and Kiyotaki (2015) and related frameworks, default arises endogenously when leverage and cash-flow risk interact with capital requirements. The novel feature is the role of liability composition: banks use long-term funding to smooth liquidity shocks and reduce rollover risk, but this same mechanism amplifies balance-sheet fragility when profitability deteriorates. In this respect, the model bridges the gap between theories of financial intermediation with default risk and the empirical patterns of pre-failure deterioration documented in the data.

Third, this paper contributes to the literature on liquidity management and debt maturity. A large body of work has examined how borrowers choose the maturity of debt to balance rollover risk and flexibility (Chatterjee and Eyigungor, 2012; Bocola and Dovis, 2019; Crouzet et al., 2016; Diamond and He, 2014). In the banking context, Choudhary and Limodio (2022) show that liquidity shocks drive banks' maturity choices, consistent with the mechanism in this paper. Here, the emphasis is on how the liability structure itself becomes a determinant of financial fragility: time deposits serve as a hedge against liquidity risk but increase exposure to default once earnings weaken.

Finally, this paper connects to the literature on bank regulation and financial stability (Corbae and D'Erasco, 2021; Begenau and Landvoigt, 2022; Lee et al., 2024). These studies emphasize the role of capital requirements and safety nets in shaping banks' risk-taking and credit supply. My framework extends this line of research by incorporating endogenous default and funding decisions in a general equilibrium environment, thereby illustrating how regulatory constraints interact with banks' liquidity management motives. The analysis offers a perspective on how regulation, funding composition, and default risk jointly influence

the resilience of the banking sector.

Overall, this paper unifies empirical evidence and quantitative modeling to show that banks' funding structures are not merely reflections of market conditions but active determinants of financial fragility. By endogenizing the evolution of funding composition within a model of limited commitment and default, it provides a framework for understanding the buildup of vulnerabilities that precede banking crises.

2. Empirical Analysis

This section provides empirical evidence on the patterns of bank behavior and performance that motivate the model developed in Section 3. I begin by describing the construction of the dataset and the sources used to measure bank-level characteristics and failures. I then document how banks' funding structures and balance sheet fundamentals evolve in the years leading up to failure, using an event-study approach that compares failing and surviving institutions. The analysis highlights two key dimensions that guide the modeling framework: the shift in funding composition toward time deposits and the joint deterioration in profitability, leverage, and credit quality preceding failure.

Data Description

I use U.S. bank-level data from the quarterly *Call Reports* filed by all insured commercial banks, and I standardize several bank-specific ratios according to the definitions provided by the Uniform Bank Performance Report (UBPR).¹ The use of the UBPR ensures consistency across banks and over time. The sample covers quarterly observations from March 2001 through March 2025.

I complement the Call Report data with the FDIC's *List of Failed Banks*, which documents all failures of FDIC-insured institutions over the same period. A bank failure is defined as either the closure of a bank by regulators or an instance of open bank assistance. Throughout my sample period, I observe 500 bank failures as reported by the FDIC.²

¹For more details on the FFIEC's UBPR and the construction of these variables, see <https://cdr.ffiec.gov/public/DownloadUBPRUserGuide.aspx>.

²For more detailed information checking my Appendix section

Fundamentals Around Bank Failures

In this section, I replicate the empirical analysis of Correia et al. (2023) to document how banks' fundamentals evolve in the periods leading up to failure, relative to banks that remain solvent. This exercise serves two purposes. First, it provides a benchmark for understanding the patterns of balance sheet deterioration that typically precede bank failures in the United States. Second, it allows me to assess how the behavior of key variables—such as capital ratios, loan growth, and funding composition—relates to the heterogeneity in banks' funding emphasized in my analysis.

To study the dynamics of funding, losses, and insolvency risk in the years preceding failure, I estimate variants of the following specification:

$$y_{j,t} = \alpha_j + \alpha_t + \sum_{k=-40}^0 \mathbb{I}_{k=t} \beta_k + \varepsilon_{j,t}, \quad (1)$$

where $y_{j,t}$ denotes a bank-level outcome, k measures the number of quarters to failure, and α_j and α_t are bank and time fixed effects, respectively. The benchmark period is set to $k = -40$, corresponding to ten years before failure, so all coefficients are measured relative to that date. The sequence of coefficients $\{\beta_k\}$ captures the average deviation of failing banks from solvent ones over time, holding constant bank-specific heterogeneity and aggregate shocks.

Funding. Figure 1 plots the evolution of banks' funding composition in the ten years preceding failure. The figure displays the estimated event-study coefficients for different categories of liabilities—checking deposits, savings deposits, time deposits, repos, and other borrowed money—relative to solvent banks, controlling for bank and time fixed effects. A clear pattern emerges: as banks approach failure, the share of time deposits rises sharply, indicating a shift toward illiquid and higher-yield liabilities. In contrast, the shares of checking and savings deposits decline steadily, reflecting a contraction in core retail funding. Repos exhibit a gradual decline, suggesting reduced use of secured short-term borrowing. Meanwhile, other borrowed money increases modestly closer to failure, reflecting a partial substitution toward unsecured wholesale funding. Together, these patterns show that as financial distress intensifies, banks substitute away from stable core deposits toward costlier and less stable wholesale funding sources.

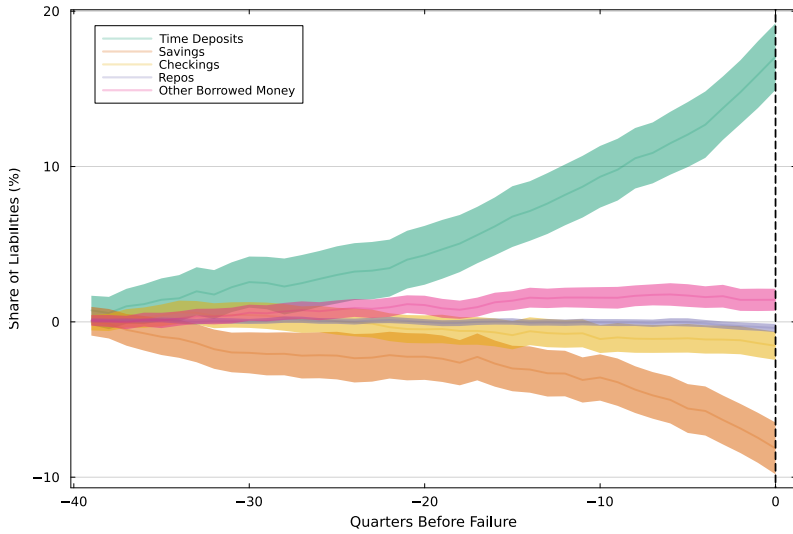


Figure 1: Funding Share Before Bank Failure

Time Deposits. Figure 2 plots the evolution of banks’ reliance on time deposits in the ten years preceding failure. The figure reports event-study coefficients for the share of time deposits in total liabilities, distinguishing between deposits above and below the FDIC insurance limit. A clear pattern emerges: as banks approach failure, the overall share of time deposits rises sharply, with the increase particularly pronounced for deposits below the insurance limit. This pattern indicates that distressed banks increasingly rely on insured retail depositors, offering higher yields to retain funding as their financial conditions deteriorate. In contrast, the share of uninsured time deposits grows more modestly, suggesting limited access to large wholesale depositors. Taken together, these results reveal a systematic shift in the composition of liabilities toward insured, longer-maturity deposits, reflecting banks’ attempts to lock in stable funding as default risk rises.

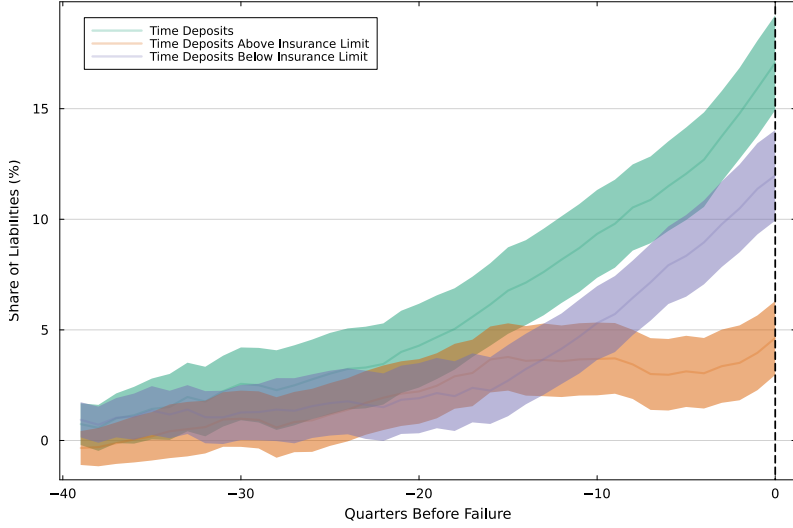


Figure 2: Funding Share of Time Deposits Before Bank Failure

Deposit Rates. Figure 3 plots the evolution of deposit rates in the ten years preceding failure. The figure reports event-study coefficients for the interest rates paid on savings and checking accounts (core deposits), time deposits, and the spread between the two. Two distinct patterns emerge. First, while both rates exhibit moderate upward trends prior to failure, the increase is markedly stronger for time deposits, whose rates rise by roughly five basis points per quarter—about twenty basis points on an annualized basis—relative to solvent banks. In contrast, interest rates on core deposits remain largely flat and eventually decline, suggesting that banks do not pass higher funding costs through to retail depositors. Second, the spread between time and core deposit rates widens substantially in the years leading up to failure, reaching over ten basis points by the quarter of failure. This widening reflects a sharp deterioration in the marginal cost of funding, as troubled banks increasingly rely on costly time deposits to attract and retain liquidity. These results highlight rising funding costs—especially for time deposits—as a key precursor to bank distress, mirroring the compositional shifts in liabilities shown in Figure 2.

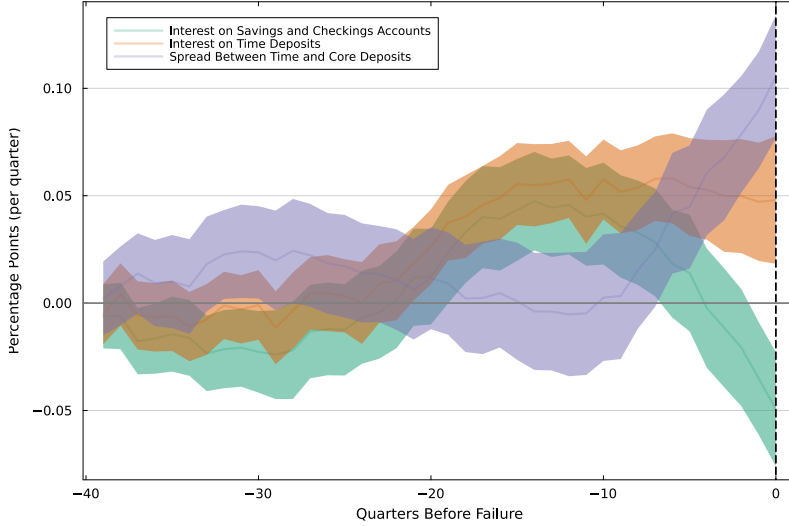


Figure 3: Deposit Rates Before Bank Failure

Because of these patterns, my modeling analysis focuses on the distinction between time deposits and checking and savings deposits, which represent two distinct forms of retail funding. Time deposits tend to increase in the periods leading up to failure, reflecting reliance on illiquid and higher-yield liabilities, while checking and savings deposits decline as banks adjust their funding structure. This distinction captures the heterogeneity in funding maturity and pricing across retail liabilities—a central mechanism in the model’s transmission of shocks to bank balance sheets.

Losses and Solvency. Figure 4 summarizes the dynamics of key bank fundamentals in the ten years preceding failure. The figure reports event-study coefficients for the net interest margin, leverage ratio, net charge-offs, and net income, estimated relative to solvent banks after controlling for bank and time fixed effects. The patterns indicate a progressive deterioration in profitability and asset performance as failure approaches. The net interest margin begins to decline about two years before failure, reflecting a narrowing gap between lending and funding rates. Leverage rises steadily throughout the period, pointing to an increase in liabilities relative to assets. Net charge-offs remain stable early on but rise sharply in the final quarters before failure, signaling mounting loan losses. Finally, net income declines persistently and turns negative several quarters before failure. Together, these patterns document a gradual weakening of earnings and asset quality leading up to

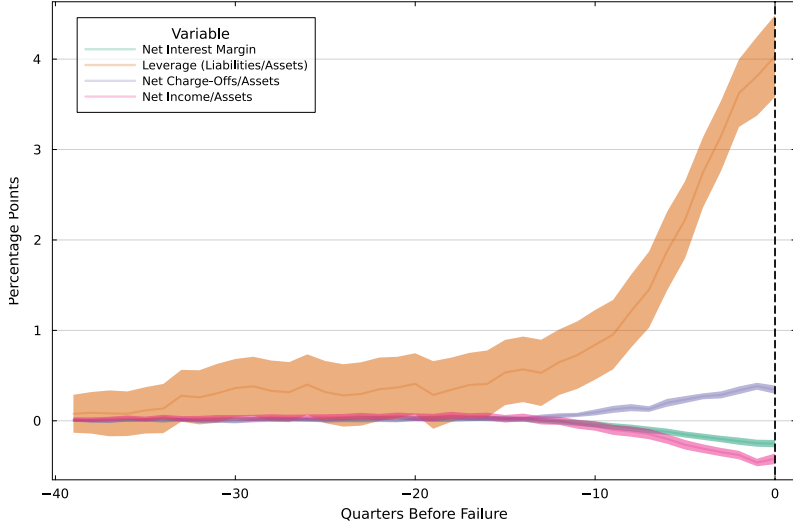


Figure 4: Losses and Solvency Before Bank Failure

bank failure.

Taken together, these findings motivate a framework in which banks' solvency evolves endogenously with profitability, funding costs, and credit losses. The steady increase in leverage and charge-offs, combined with the decline in net interest margins and net income, suggests that both earnings compression and loss realization play central roles in the buildup to failure. In the model that follows, I formalize these mechanisms by allowing banks' balance sheets to respond to shocks that affect their funding costs and loan returns, shaping the evolution of their net worth and default risk.³

The empirical evidence presented in this section reveals two central patterns that guide the theoretical analysis. First, banks approaching failure experience a marked reallocation of funding toward time deposits and other costly liabilities, accompanied by a decline in core deposits. Second, profitability, leverage, and credit performance deteriorate steadily in the years preceding failure, with losses and higher funding costs jointly eroding net income. These findings point to a close interaction between banks' funding structures and their solvency dynamics. In the next section, I develop a model that formalizes these mechanisms,

³In Appendix Figure A.1, I show that the increase in time deposits—which would imply an increase in the maturity of banks' liabilities—is not matched by an increase in the maturity of their assets. In fact, asset maturity declines, implying that the exposure to interest rate risk of banks closer to failure actually decreases.

allowing funding composition, lending returns, and default risk to co-evolve within a unified framework.

3. Model

This section develops a model of financial intermediation to study how banks' financial frictions interact with their endogenous default decisions. The framework features entrepreneurs seeking external financing for risky projects, competitive households allocating savings across assets, and banks that intermediate funds between the two sectors. The interplay between imperfect competition, regulatory constraints, and wholesale funding frictions generates the dynamics observed in the periods preceding bank failure.

Entrepreneurs face a static discrete choice problem when deciding whether to finance a risky project through bank borrowing. Households are competitive and can save either in deposits or in long-term bank liabilities. Banks act as intermediaries by accepting funds from households and extending loans to entrepreneurs. The economy produces a single final good, and all variables are expressed in units of consumption of this good.

Banks face several frictions that govern their funding life cycle. First, imperfect competition in the loan market allows banks to set lending rates to maximize profits. Second, regulatory constraints impose capital requirements that compel banks to manage their lending and funding decisions intertemporally, maintaining sufficient cash buffers against potential capital shortfalls. Third, time deposits represent a more costly funding source, reflecting both their longer maturity and greater exposure to default risk.

Households

The economy features a representative household whose lifetime utility is given by

$$E_0 \left[\sum_{t=0}^{\infty} \beta^t \log(C_t) \right].$$

where β is the discount factor and C_t is their consumption. The household owns all banks in the economy. I study the perfect foresight transition paths with respect to aggregate states, so the stochastic discount factor and the real interest rate are linked through the

Euler equation for savings, $\Lambda_{t+1} = \frac{1}{R_{f,t}}$, where $R_{f,t}$ is the risk-free rate set by the monetary authority.

The household supplies labor to firms at wages W_t and rents capital via entrepreneurs. The household has a limited supply of labor $\bar{L} = 1$. It also saves by buying deposits, D , and certificates of deposits, B , from banks. They receive dividends from the banks and are taxed lump-sum. They fund new banks by transferring some equity, denoted by \bar{n} , so they can start their operation.

Firms

The economy is populated by a representative final-good firm that rents capital from entrepreneurs at rate $R_{K,t}$ and hires labor at wage W_t to operate a constant-returns-to-scale production technology:

$$Y_t = \bar{p}_t K_t^\alpha L_t^{1-\alpha}, \quad (2)$$

where \bar{p}_t represents an aggregate *capital-quality shock* that affects both the productivity of capital and the expected success rate of entrepreneurial projects.

The firm's static profit-maximization problem is

$$\max_{K_t, L_t} \bar{p}_t K_t^\alpha L_t^{1-\alpha} - W_t L_t - R_{K,t} K_t. \quad (3)$$

The first-order conditions imply:

$$W_t = (1 - \alpha) \bar{p}_t \left(\frac{K_t}{L_t} \right)^\alpha, \quad (4)$$

$$R_{K,t} = \alpha \bar{p}_t \left(\frac{L_t}{K_t} \right)^{1-\alpha}. \quad (5)$$

Assuming labor supply is normalized to $L_t = 1$, equilibrium wages and the rental rate of capital are

$$W_t = (1 - \alpha) \bar{p}_t K_t^\alpha, \quad (6)$$

$$R_{K,t} = \alpha \bar{p}_t K_t^{\alpha-1}. \quad (7)$$

The rental rate $R_{K,t}$ determines the aggregate return to capital paid to entrepreneurs. Consistent with the entrepreneurial problem described below, the gross return on entrepreneurs' capital claims is given by:

$$R_{E,t+1} = \frac{R_{K,t+1}}{\bar{p}_t} + (1 - \delta) = \alpha K_t^{\alpha-1} + (1 - \delta), \quad (8)$$

where $(1 - \delta)$ denotes the resale value of undepreciated capital. This formulation captures that when the quality of capital, \bar{p}_t , is high, the effective return received by entrepreneurs—normalized by capital quality—remains unchanged. Hence, only the firm's production technology depends on the aggregate capital-quality shock \bar{p}_t .

This relationship arises because entrepreneurs are subject to limited liability and may default on their obligations. As a result, the aggregate return to entrepreneurial capital is determined solely by the production technology and the effective depreciation of assets, rather than by the realized capital quality itself. The role of limited liability in implying this outcome will become clearer in the next subsection.

Entrepreneurs

The entrepreneurial sector consists of two-period entrepreneurs who finance investment through bank loans. Each entrepreneur belongs to a distinct bank pool, and there is no interbank competition or mobility across pools. The set of entrepreneurs linked to bank j constitutes its *client pool*, capturing the bank's local market power, consistent with recent empirical evidence.

Each pool contains a unit mass of entrepreneurs indexed by $i \in [0, 1]$. Entrepreneurs are risk-neutral and maximize expected profits, which are ultimately transferred to the household sector.

In period t , each entrepreneur borrows \bar{k} units of the final good from a bank to purchase risky capital claims priced at Q_t . Hence,

$$k_t^i = \bar{k}.$$

The capital claim yields a stochastic return per unit of loan given by:

$$R_{E,t+1} = \alpha K_t^{\alpha-1} + (1 - \delta),$$

where $\alpha K_t^{\alpha-1}$ is the aggregate rental rate of capital determined by firms—abstracting from the quality shock—and $(1 - \delta)$ represents the resale value of undepreciated capital. If the project succeeds, entrepreneurs receive this gross return; if it fails, the payoff is zero due to limited liability. Thus, the realized return on entrepreneurs' capital claims depends on the project's success state, while the expected return reflects both the production technology and the probability of repayment.

Each entrepreneur draws an idiosyncratic return x_t^i upon investment success, which is private information and expressed as a share of the borrowed amount \bar{k} . Banks cannot observe x_t^i ex ante and therefore charge a uniform loan rate within each pool. The realization of x_t^i is known to entrepreneurs at the beginning of period t .

Suppose entrepreneur i belongs to bank j 's client pool, which faces a common project success probability $p_{t+1}^j(z_{t+1}, x_t^*)$. The variable z_{t+1} denotes a *bank-specific state*, capturing idiosyncratic credit risk conditions or shocks to bank j 's balance sheet. The function $p_{t+1}^j(z_{t+1}, x_t^*)$ represents the probability that projects financed by bank j succeed, conditional on its state z_{t+1} and on the cutoff entrepreneur x_t^* . The cutoff x_t^* reflects the risk composition of the bank's loan portfolio: when the marginal project offers higher expected returns, it also entails greater risk, thereby lowering the pool's overall success probability. Aggregating across the continuum of banks, the economy-wide success probability is given by the mass-weighted average

$$\bar{p}_{t+1} = \int_0^1 p_{t+1}^j(z_{t+1}^j, x_t^{j*}) d\mu^j,$$

which represents the expected share of successful projects in the aggregate banking system.

The project's gross return per unit of loan is therefore:

$$\begin{cases} R_{E,t+1} + x_t^i, & \text{with probability } p_{t+1}^j(z_{t+1}, x_t^*), \\ 0, & \text{with probability } 1 - p_{t+1}^j(z_{t+1}, x_t^*). \end{cases} \quad (9)$$

The gross return is $R_{E,t+1} + x_t^i$ in the successful state and 0 in failure, implying full loss of capital.⁴ The success probability $p_{t+1}^j(z_{t+1}, x_t^*)$ is i.i.d. across entrepreneurs within a pool but correlated across time through the evolution of z_{t+1} .⁵ The failure rate within each pool is $1 - p_{t+1}^j(z_{t+1}, x_t^*)$, and aggregation across all banks yields the unconditional failure probability $1 - \bar{p}_{t+1}$.

Entrepreneurs cannot switch across banks. Given the loan rate $R_{\ell,t}^j$, each entrepreneur decides whether to borrow and invest. They must repay $R_{\ell,t}^j$ if they borrow, and due to limited liability, their payoff is bounded below by zero. Table 1 summarizes the payoff structure.

Table 1: Entrepreneur's Problem (conditional on investing)

State	Receive	Pay	Probability
Success	$R_{E,t+1} + x_t^i$	$R_{\ell,t}^j$	$p_{t+1}^j(z_{t+1}, x_t^*)$
Failure	0	0	$1 - p_{t+1}^j(z_{t+1}, x_t^*)$

Since $R_{\ell,t}^j > 1$, entrepreneurs cannot repay if their project fails, and the bank seizes the remaining capital claim, which has zero value.

The expected payoff of entrepreneur i conditional on borrowing at rate $R_{\ell,t}^j$ is

$$\pi_t(R_{\ell,t}^j) = E_t[p_{t+1}^j(z_{t+1}, x_t^*) (R_{E,t+1} - R_{\ell,t}^j + x_t^i) \bar{k}].$$

If entrepreneurs do not invest, they forgo x_t^i . Hence, their decision rule is

$$U^e = \max_{h \in \{0,1\}} h \pi_t(R_{\ell,t}^j),$$

where h is the binary investment choice. An entrepreneur invests if and only if

$$R_{E,t+1} + x_t^i \geq R_{\ell,t}^j, \quad (10)$$

i.e., when the expected project return exceeds the loan rate.

⁴This setup maps to Coimbra and Rey (2024), where capital return equals $R_{K,t} + (1 - \delta)$. I interpret \bar{p}_t as an aggregate capital-quality shock, with an increased credit risk component as Corbae and D'Erasco (2021).

⁵This structure parallels Vasicek (2002), often used in regulatory credit-risk modeling.

Loan Demand. With no interbank competition or mobility, each bank j faces a unique loan demand function. From the investment rule in Equation 10 and the distribution of x_t^i , loan demand per unit of capital is

$$\ell^d(R_{\ell,t}^j, R_{E,t+1}) = \Pr(x_t^i \geq R_{\ell,t}^j - R_{E,t+1}) \bar{k}. \quad (11)$$

The marginal entrepreneur is defined by the indifference condition $x_t^* = R_{\ell,t}^j - R_{E,t+1}$. Since x_t^i follows a known distribution, the loan demand corresponds to the complementary cumulative distribution function of x_t^i evaluated at x_t^* . Thus, loan demand increases with $R_{E,t+1}$ and decreases with $R_{\ell,t}^j$: higher project returns or lower lending rates raise the share of entrepreneurs willing to invest.

Banks

There is a continuum of banks of measure one, indexed by $j \in [0, 1]$, all owned by the representative household. Each bank is operated by a manager who makes decisions regarding entry, default, lending, and funding. The manager seeks to maximize the expected discounted stream of dividend payments, div_t , according to the objective function:

$$E_0 \left[\sum_{t=0}^{\infty} \sigma^t \Lambda_t, div_t \right],$$

where Λ_t denotes the household's stochastic discount factor and $\sigma \in (0, 1]$ captures the manager's degree of myopia. When $\sigma < 1$, managerial myopia introduces a potential agency friction between the bank manager and the household, as in Corbae and D'Erasco (2021). To ensure a well-defined cross-sectional distribution of banks, I impose the condition $\sigma \Lambda_{t+1} R_{f,t} < 1$, which is standard in incomplete market environments. Here, $R_{f,t}$ denotes the risk-free rate.

Assets. To model bank solvency risk, I begin by characterizing the composition of bank assets. Each bank invests in loans that yield an agreed-upon gross interest rate $R_{\ell,t}^j$. Let ℓ_{t-1}^j denote the stock of loans extended by bank j in period $t - 1$ at rate $R_{\ell,t-1}^j$. The value of bank j 's assets at time t is given by:

$$a_t^j = p(z_t^j, R_{\ell,t-1}^j - R_{E,t+1}) R_{\ell,t-1}^j \ell_{t-1}^j, \quad (12)$$

where $p(\cdot)$ is the fraction of performing loans that are repaid. Defaulted loans are realized as losses on the bank's balance sheet, and $1 - p(\cdot)$ represents the share of charge-offs. I assume that z_t^j follows a persistent AR(1) process, capturing cyclical variation in credit risk across banks.

Resources. Bankers use their cash-on-hand (n), deposits (d), and time deposits (b) to finance new loans $\ell(R_{\ell,t}^j, R_{E,t+1})$ at the interest rate $R_{\ell,t}^j$.

Time deposits are long-term instruments that do not fully mature within a single period. A fraction λ of their principal is repaid each period, while the remaining share $1 - \lambda$ remains outstanding. Debt holders receive a coupon payment c on the outstanding amount. Deposits, in contrast, are short-term contracts that fully mature each period.

Given their liabilities and loan portfolio, a bank's cash-on-hand evolves according to:

$$n_t^j = a_t^j - \omega_t^j \ell_t^j - d_t^j - (\lambda + c)b_t^j. \quad (13)$$

Here, a_t^j denotes the value of bank j 's assets, ω_t^j is an idiosyncratic shock affecting the revenue generated from those assets, d_t^j represents deposit payouts inherited from the previous period, and $(\lambda + c)b_t^j$ corresponds to repayments on maturing time deposits plus coupon payments.

The idiosyncratic shock ω_t^j introduces cross-sectional heterogeneity across banks, following the approach of Ottonegro and Winberry (2020). This shock also helps match the empirical distribution of default rates observed in the data. I assume that ω_t^j is independently and identically distributed across banks and time, following a normal distribution, $\omega_t^j \sim N(0, \eta_\omega^2)$. Intuitively, ω_t^j captures fluctuations in asset returns—such as unrealized revenue losses from non-performing loans—that generate liquidity needs at the bank level.

Equity. At the beginning of each period, the bank's book equity is defined as the value of its cash-on-hand net of the outstanding amount of long-term debt, discounted at its present value:

$$e_t^j = n_t^j - q_{b,t}^{rf}(1 - \lambda)b_t^j, \quad (14)$$

where $q_{b,t}^{rf}$ denotes the risk-free price of long-term liabilities.

This specification implies that when equity is evaluated at fair value, the bank's liabilities are also marked to fair value rather than to market value. This assumption is consistent

with the regulatory treatment of Tier 1 capital, under which banks may include unrealized gains from changes in the fair value of their liabilities, excluding those arising from their own credit risk. Consequently, discrepancies can emerge between the fair value and the market value of equity.

Resource Constraint. Banks use their cash-on-hand and liability issuance to finance new lending, giving rise to the following per-period resource constraint:

$$div_t^j + \ell^d(R_{\ell,t}^j, R_{E,t+1}) = n_t^j + q_{d,t}d_{t+1}^j + q_{b,t}(b_{t+1}^j - (1 - \lambda)b_t^j) - \psi - Z(d_{t+1}^j, b_{t+1}^j, b_t^j). \quad (15)$$

Equation (15) describes the bank's flow-of-funds constraint. On the left-hand side, dividends div_t^j and new lending $\ell^d(R_{\ell,t}^j, R_{E,t+1})$ represent the uses of funds. The loan demand function $\ell^d(\cdot)$ is derived from the entrepreneurs' problem and links the bank-specific lending rate $R_{\ell,t}^j$ to the expected return on entrepreneurial projects $R_{E,t+1}$ (see Equation 11).

On the right-hand side, n_t^j denotes the bank's net worth entering the period. The terms $q_{d,t}d_{t+1}^j$ and $q_{b,t}(b_{t+1}^j - (1 - \lambda)b_t^j)$ capture the funds raised through deposits and time deposits, respectively. The expression $b_{t+1}^j - (1 - \lambda)b_t^j$ corresponds to the net issuance of time deposits, where λ is the maturity parameter governing the fraction of long-term liabilities that expires each period.

Debt issuance entails convex costs captured by

$$Z(d_{t+1}^j, b_{t+1}^j, b_t^j) = \zeta (d_{t+1}^j)^2 + \zeta (b_{t+1}^j - (1 - \lambda)b_t^j)^2,$$

where $\zeta > 0$ measures the marginal cost of issuing both short- and long-term debt. The fixed operating cost $\psi > 0$ reflects overhead necessary to maintain banking operations.

Taken together, these components characterize how each bank finances its lending activity, covers operating costs, and distributes dividends to shareholders.

In addition, I assume that banks cannot repurchase their outstanding stock of time deposits, i.e.,

$$b_{t+1}^j - (1 - \lambda)b_t^j > 0.$$

Using the cash-on-hand equation 13 and fair value equity 14, we can determine next period

equity by ⁶

$$e_{t+1}^j = a_{t+1}^j - d_{t+1}^j - (\lambda + c + (1 - \lambda)q_{b,t+1}^{rf})b_{t+1}^j.$$

A key friction in the model is the assumption that banks are unable to issue equity, which necessitates that dividends must always be non-negative, expressed as:

$$div_t^j \geq 0.$$

This constraint prevents banks from raising equity to substitute deposits or long-term liabilities for funding their lending activities. Additionally, it highlights the limited liability of banks, as they have the option to default on their debt, resulting in equity holders losing their entire investment.

The next important ingredient in my model is regulation, namely, capital requirement

$$e_{t+1}^j \geq \kappa a_{t+1}^j. \quad (16)$$

Equation 16 implies that the bank's fair value equity at the beginning of the next period has to be no smaller than a fraction κ of their total asset. Due to the no-equity investment and the capital constraints, banks will need to smooth their cash-holding to avoid states with low liquidity and, thus, default.

Lastly, I follow Title 12 (“Banks and Banking”) of the *Code of Federal Regulations*, which stipulates that proposed dividends cannot exceed a bank’s net income. Accordingly, dividends are restricted by

$$div_t^j \leq E_{z_{t+1}|z_t}[\Pi_{t+1}],$$

where $\Pi_{t+1} = a_{t+1} - \ell_t$ represents the interest payment on the loans tomorrow. A similar assumption is made by Corbae and D’Erasco (2021). In this setup, the restriction ensures that the bank’s value function remains bounded and concave.

Lastly, notice that all constraints are linear on the constant \bar{k} . Therefore, we can normalize

⁶Here I am implicitly assuming that revenue shock, for example, unrealized losses from non-performing loans, does not interact with the requirements over capital tomorrow. This is in line with the reporting on capital tier ratio from Schedule RC-R, for which only unrealized losses on securities and debt securities are accounted.

all variables at the bank level by \bar{k} . Consequently, to solve the bank problem, we are only required to know aggregate variable $R_{E,t+1}$ in the steady state. As a simplification to speed up the computational process, I calibrate the steady $R_{E,t+1}$ to match the banks' net interest margins, while \bar{k} is obtained as a residual of the entrepreneur return.

Debt Pricing

Households competitively lend resources to banks at the price schedules $q_d(z_t, R_{\ell,t}, d_{t+1}, b_{t+1})$ and $q_b(z_t, R_{\ell,t}, d_{t+1}, b_{t+1})$.

Banks cannot distinguish between the types of debt on which they default. If they default on deposits, they must also default on time deposits, and vice versa. The default decision of bank j is denoted by $h(z_t, n_t, b_t)$, where (z_t, n_t, b_t) are the bank's state variables.

A key distinction between deposits and time deposits arises from the presence of deposit insurance. Since, on average, roughly half of time deposits exceed the insurance limit, they are more exposed to default risk. To capture this feature, I assume a repayment hierarchy that guarantees the repayment of depositors before time deposit holders in the event of default.⁷

The process unfolds as follows. Whenever a bank defaults, debt holders take control of the bank's assets. Assets are liquidated with a recovery rate $\gamma \in (0, 1)$. Depositors are paid first, and any remaining funds after covering deposits are distributed to time deposit holders, who receive

$$\max\{0, \gamma(a_t - \omega_t \ell_t) - d_t\}.$$

Banks are required to pay insurance premiums to a regulator, net of the expected recovery on assets. The insurance premium is fairly priced, taking into account the bank's lending, debt, and default decisions. Consequently, deposits are priced net of this insurance premium. After liquidation, any unrecovered portion of assets is transferred lump-sum to the household sector; thus, there is no aggregate welfare loss from default.

Since households hold these liabilities, they discount them using the stochastic discount

⁷This assumption follows the hierarchy of claims established by the FDIC.

factor Λ_t . The price of deposits, net of the insurance premium, is therefore given by:

$$q_d(z_t, R_{\ell,t}, d_{t+1}, b_{t+1}) = E_t \{ \Lambda_{t+1} [1 - h(z_{t+1}, n_{t+1}, b_{t+1}) \\ + h(z_{t+1}, n_{t+1}, b_{t+1}) \min\{1, \gamma(a_{t+1} - \omega_{t+1}l_{t+1})/d_{t+1}\}] \}.$$

Similarly, the price of time deposits is given by:

$$q_b(z_t, R_{\ell,t}, d_{t+1}, b_{t+1}) = E_t \{ \Lambda_{t+1} [(1 - h(z_{t+1}, n_{t+1}, b_{t+1}))(\lambda + c + (1 - \lambda)q_{b,t+1}) \\ + h(z_{t+1}, n_{t+1}, b_{t+1}) \min \left\{ c + \lambda + (1 - \lambda)q_{b,t}^{rf}, \frac{\max\{0, \gamma(a_{t+1} - \omega_{t+1}l_{t+1}) - d_{t+1}\}}{b_{t+1}} \right\} \] \},$$

where $q_{b,t+1}$ denotes the price of time deposits next period.

Bankers' Recursive Problem

Since the banker's problem is identical across banks, I drop the index j . The state vector (z, n, b) summarizes the bank's relevant variables: the idiosyncratic shock to the share of performing loans z , cash-on-hand n , and outstanding wholesale debt b . Bankers lack commitment and may default on their debt obligations. The value of operating the bank is therefore given by:

$$V(z, n, b) = \max_{h \in \{0,1\}} (1 - h) V^c(z, n, b),$$

where h is the default indicator, $h(z, n, b)$ denotes the corresponding default rule, and $V^c(\cdot)$ represents the continuation value of remaining solvent. If the banker defaults, the value is zero.

The continuation value satisfies the following recursive problem:

$$\begin{aligned}
V^c(z, n, b) &= \max_{R_\ell, d', b'} \left\{ \text{div} + E_{z'|z} [\sigma \Lambda_{t+1} V(p', n', b')] \right\} \\
\text{s.t. } \text{div} &= n - \ell^d(R_\ell, R'_E) - \psi + q_d d' + q_b(b' - (1 - \lambda)b) - Z(d', b', b) \geq 0, \\
a' &= p(z', R_\ell - R'_E) R_\ell \ell^d(R_\ell, R'_E), \\
e' &\geq \kappa a', \\
e' &= a' - d' - (\lambda + c + (1 - \lambda)q_b^{rf})b', \\
n' &= a' - \omega' \ell^d(R_\ell, R'_E) - d' - (\lambda + c)b', \\
b' - (1 - \lambda)b &\geq 0, \\
\text{div} &\leq E_{z'|z} [a' - \ell^d(R_\ell, R'_E)].
\end{aligned}$$

The bank chooses its loan rate R_ℓ , deposit issuance d' , and long-term debt b' to maximize its expected discounted value, subject to the non-negativity of dividends, regulatory capital requirements, and the law of motion for assets and equity. All expectations are conditional on the current loan-performance state z .

Default Characterization

Banks face the possibility of default whenever their continuation value becomes non-positive. Because dividend payments must be non-negative, the continuation value $V^c(z, n, b)$ is positive for any feasible combination of (z, n, b) that satisfies the resource and feasibility constraints. When these constraints cannot be met—due to insufficient net worth or excessive leverage—the bank optimally defaults.

Formally, let Ω denote the set of feasible states. The *default region* is defined as:

$$\mathcal{H} = \{(z, n, b) \in \Omega : V^c(z, n, b) \leq 0\}.$$

In this region, the value of continuing operations falls below zero, and the banker chooses to default. Default implies liquidation of the bank and a payoff of zero to the banker, reflecting limited liability.

Hence, the bank's overall value function satisfies:

$$V(z, n, b) = \max\{V^c(z, n, b), 0\},$$

where $V^c(z, n, b)$ denotes the value of continuing operations and the zero value represents default. The boundary between the continuation and default regions defines the *endogenous default threshold*, which determines the states under which a bank remains solvent.

Finally, default occurs only when the continuation value $V^c(z, n, b)$ is *not feasible*, i.e., when no combination of (R_ℓ, d', b') satisfies the resource and feasibility constraints while maintaining non-negative dividends. In such cases, the bank cannot continue operations, and default becomes the only admissible outcome.

The banking sector features endogenous exit through default and immediate entry of replacement banks, guaranteeing a stationary distribution of banks. A full characterization of the distributional law of motion and the stationary competitive equilibrium is provided in Appendix B.

4. Quantitative Analysis

In this section, I examine the quantitative implications of the model developed in Section 3. The goal is to assess whether the framework can replicate key features of the U.S. banking sector and generate realistic differences in banks' balance sheets and performance.

The analysis proceeds in three steps. First, I calibrate the model to match targeted moments that describe the empirical distribution of bank characteristics, such as leverage, funding composition, and profitability. Second, I assess the model's ability to reproduce untargeted life-cycle dynamics before default, comparing simulated patterns of leverage, funding, and profitability with those observed in the data. Finally, I conduct counterfactual exercises to study how funding structure and capital regulation influence banks' risk, funding choices, and stability.

Overall, these exercises show that the model captures important aspects of balance-sheet heterogeneity and bank fragility, providing a useful framework for analyzing the interaction between funding, default risk, and regulation.

Computation

The model described in Section 3 features heterogeneity across banks and important nonlinearities. All nonlinearities arise from the bank’s problem due to the endogenous default decision and the sometimes binding constraints. Due to these nonlinearities, I rely on global methods to solve the model (value function iteration).

Even after reducing the problem to a stationary equilibrium, the model features three individual state variables at the bank level: (z, n, b) and three choice variables (R_ℓ, d', b') and is therefore subject to the curse of dimensionality.⁸ The algorithm for solving the model relies on graphics processing units (GPUs) to highly parallelize the solution.

Parameterization

The model calibration proceeds in two steps. First, a subset of parameters is directly obtained from the data, while the remaining parameters are estimated using the Simulated Method of Moments (SMM). As discussed later, the selected set of moments is chosen to capture the key financial frictions faced by banks. Throughout, one model period corresponds to a quarter, so all parameters and targets are expressed at a quarterly frequency.

The primary data source is the FFIEC *Call Reports*. I begin by parameterizing the stochastic process for loan losses.⁹ Let $\text{nco}_{j,t}$ denote net loan charge-offs divided by total loans for bank j at time t , and define the implied loan-survival share

$$p_{j,t} \equiv 1 - \text{nco}_{j,t} \in (0, 1].$$

I estimate a linear regression of $\log p_{j,t}$:

$$\log p_{j,t} = \mu_p + \rho_p \log p_{j,t-1} + u_{j,t}, \quad u_{j,t} \sim \mathcal{N}(0, \eta_p^2),$$

Given (μ_p, ρ_p, η_p) , I discretize the latent AR(1) process using Tauchen (1986) on the $\log p$ scale and map back to $p = \exp(\cdot)$, truncating the support to $p \leq 1$ and $p \geq \varepsilon$.

⁸In the Appendix C, I cover how I compute the policies and steady-state distribution of banks.

⁹For consistency with the model, I use a subsample of my data for banks that realize losses at least 95% of their sample.

An essential parameter for the model is the average maturity of time deposits. Following the literature, I assume a maturity of one year, which implies $\lambda = 1/4$ in quarterly terms.

The loan demand function is parameterized by assuming that the idiosyncratic component x_t^i follows a logistic distribution, yielding

$$\ell^d(R_{\ell,t}, R_{E,t+1}) = \frac{1}{1 + \exp[\theta(R_{\ell,t} - R_{E,t+1})]}, \quad (17)$$

where θ captures the sensitivity of loan demand to the lending rate and $R_{E,t+1}$ is the expected return on capital.¹⁰ Parameters θ and $R_{E,*}$ are endogenously determined in the steady state, while \bar{k} is recovered residually from the steady-state capital return condition using the aggregate loan supply.

Intuitively, higher asset returns increase the incentive to invest, raising the demand for loans. Under the logistic specification, loan demand becomes less sensitive to loan rates when lending rates are already high. Because the aggregate loan supply is tied to the asset price, a contraction in loan supply reduces the asset price and shifts loan demand upward, partially offsetting the initial decline.

The remaining parameters are calibrated directly from macro-financial data. The aggregate risk-free rate is set to the average effective federal funds rate between 2002 and 2023, excluding observations below 20 basis points per year. The recovery rate on assets is set to $\gamma = 0.70$, slightly higher than the 51–55% range reported by Correia et al. (2023), but consistent with Corbae and D’Erasco (2021). The capital requirement ratio is fixed at $\kappa = 0.06$, matching the average Tier 1 capital ratio. The capital share α is set to 0.35, following standard values in the macro-finance literature, and the depreciation rate $\delta = 0.05$ implies an average loan maturity of five years.¹¹ The coupon rate c is set such that in a risk-free environment both deposits and time deposit yield the same interest rate. Table 2 summarizes the externally calibrated parameters.

¹⁰This representation of loan demand is similar to those in Wang et al. (2022) and Jiang (2023), with the difference that the return on capital is aggregate rather than idiosyncratic. A similar form can be obtained under linear utility with a GEV shock.

¹¹Geelen et al. (2024) document that debt maturity is positively correlated with asset life, as firms tend to match the maturity of assets and liabilities.

Table 2: Fixed Parameters

Parameter	Symbol / Value	Source / Target
Capital share	$\alpha = 0.35$	Standard in literature
Depreciation rate	$\delta = 0.050$	Implies average loan maturity of 5 years
Risk-free rate (quarterly)	$R_f = 1.006$	Avg. Fed Funds rate (2001–2025)
Recovery rate on assets	$\gamma = 0.7$	Corbae and D’Erasco (2021)
Capital requirement ratio	$\kappa = 0.06$	Tier 1 capital ratio
Time deposit maturity	$\lambda = 1/4$	One-year maturity assumption

Notes: Parameters in this table are externally fixed prior to the simulated method of moments (SMM) estimation. One model period corresponds to a quarter.

Targeted Moments

In this subsection, I assess whether the model can accurately approximate the targeted and untargeted moments. I begin by describing the endogenously calibrated parameters in the steady state, then discuss the targeted moments and their mapping to key bank frictions, and finally evaluate the model’s fit and external validity.

Table 3 reports the parameters calibrated within the model. Because competition across banks is limited, the parameter governing the interest rate sensitivity of loan demand, θ , is higher than the value estimated by Wang et al. (2022). The steady-state entrepreneurial return, $R_{E,*}$, plays a key role in matching the net interest margin, as it determines the level of the average lending rate. The myopia parameter, σ , is close to the value in Corbae and D’Erasco (2021), which helps generate leverage ratios consistent with those observed in the data. The fixed operating cost, ψ , corresponds to approximately 0.04% of average lending in the steady state, or about 0.4% of banks’ equity. The parameters that govern default behavior, ψ and η_ω , are identified jointly in the calibration. Finally, the issuance cost of deposits, ζ , governs the equilibrium share of time deposits in total funding.

The targeted moments are chosen to reflect the key frictions that banks face in the model. Because banks operate in imperfectly competitive markets, their lending rates depend on the elasticity of loan demand. To capture this relationship, I target the empirical net interest margin (NIM), defined as the difference between interest income and interest expense divided by total assets. This moment summarizes banks’ average markup over funding costs and

Table 3: Targeted Parameters

Parameter	Description	Calibrated Value
θ	Interest rate sensitivity	301
$\eta\omega$	Std. dev. of loan shock	0.03
σ	Manager myopia	0.975
ψ	Fixed operating cost (as share of \bar{k})	2×10^{-4}
ζ	Debt Issuance cost	25×10^{-4}
$R_{E,*}$	Steady-state entrepreneurial return	1.085

Note: Parameters are calibrated to match the empirical moments reported in Table 4. $R_{E,*}$ denotes the steady-state equilibrium return on equity, and c corresponds to the coupon rate on time deposits. All parameters are expressed in quarterly terms unless otherwise noted.

disciplines the parameter θ , which governs the sensitivity of loan demand to interest rate changes—particularly when banks adjust their funding composition toward more costly time deposits.

A second key friction arises from the banks' exposure to default risk. While insured deposits are protected by the FDIC, time deposits are not, and thus carry an endogenous default premium. I measure this premium as the spread between rates on time deposits and savings and checking accounts, which serves as a moment capturing the equilibrium default risk in the model. Additionally, the observed failure rate of banks provides an aggregate indicator of default risk and is included among the targets.

The final set of moments captures banks' funding and leverage decisions. Banks can finance themselves through retained earnings or external liabilities, subject to regulatory and market constraints. I therefore target the average leverage ratio, which provide information about the tightness of these constraints. To discipline the model's funding structure, I target the mean and dispersion of the share of time deposits in total liabilities, which reflects banks' composition between illiquid and liquid funding.

Table 4 compares the model-implied and empirical moments. Overall, the model fits the data well. It closely matches the margins observed in the data and reproduces the average leverage ratio and its volatility. The spread between time and core deposit rates is slightly

Table 4: Targeted Moments: Data vs. Model

Moment	Data (%)			Model (%)		
	Mean	Std. Dev.	—	Mean	Std. Dev.	—
Share of failing banks	0.079	—	0.084	—	—	—
Leverage	89.53	—	87.34	—	—	—
Share of time deposits	36.70	15.88	35.05	11.59	—	—
Net interest margin	0.89	—	1.03	—	—	—
Spread btwn. time dep. and deposit	0.37	—	0.34	—	—	—

Note: Empirical moments are computed from FFIEC Call Reports (2001–2025). Model moments correspond to the stationary equilibrium of the calibrated economy. All variables are expressed as percentages. Standard deviations are in percentage points.

larger in the model—about 4 basis points above the data—consistent with possibly a smaller coupon in the model. The share of time deposits funding and its standard deviation are also well captured, indicating that the model successfully reproduces the heterogeneity in banks' funding composition.

The model's ability to match both the average levels and dispersion of leverage, funding composition, and pricing spreads supports its quantitative relevance. In the next subsection, I evaluate the model's untargeted moments, which provide an additional validation of its capacity to capture banks' dynamic responses to shocks.

Untargeted Moments - Dynamics Around Default

The analysis of untargeted moments provides a complementary validation of the model's performance beyond the steady-state calibration. While the targeted moments ensure that the model matches key cross-sectional averages, the untargeted moments assess whether it can replicate the dynamic patterns observed in the data as banks approach default. In particular, I examine how leverage, profitability, and funding composition evolve in the simulated economy around episodes of bank failure. These dynamics are then compared to the empirical event-study patterns documented in Section 2, providing a test of whether the model captures the buildup of fragility that precedes default.

Leverage Dynamics. Figure 5 compares the evolution of leverage ratios in the data and in the simulated model around episodes of bank failure. Both series display a gradual and persistent increase in leverage in the years preceding default, reflecting the buildup of balance-sheet risk as banks accumulate liabilities relative to assets. The model closely tracks the empirical pattern, reproducing both the slow upward drift and the acceleration in leverage in the final quarters before failure. This close alignment suggests that the mechanisms governing funding decisions and default in the model successfully capture the gradual deterioration in banks' solvency observed in the data.

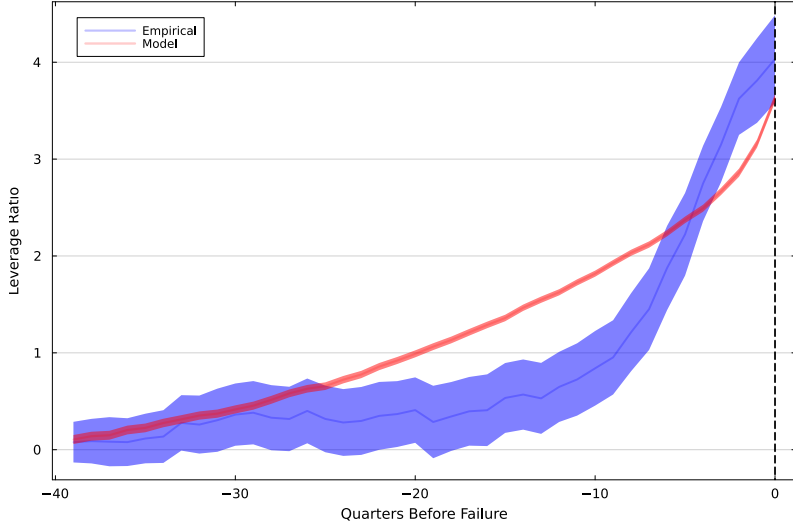


Figure 5: Leverage (Total Liabilities/Total Assets) Before Bank Failure

Funding Dynamics. Figure 6 compares the evolution of time deposits, expressed as a share of total liabilities, in the data and in the simulated model around episodes of bank failure. Both series show a gradual and sustained increase in the share of time deposits as default approaches, indicating that banks progressively shift toward illiquid and higher-yield funding sources when facing distress. The model captures both the timing and magnitude of this buildup, closely mirroring the empirical pattern. This alignment suggests that the mechanisms linking funding costs, funding choice, and solvency in the model successfully reproduce the compositional changes in liabilities observed prior to failure.

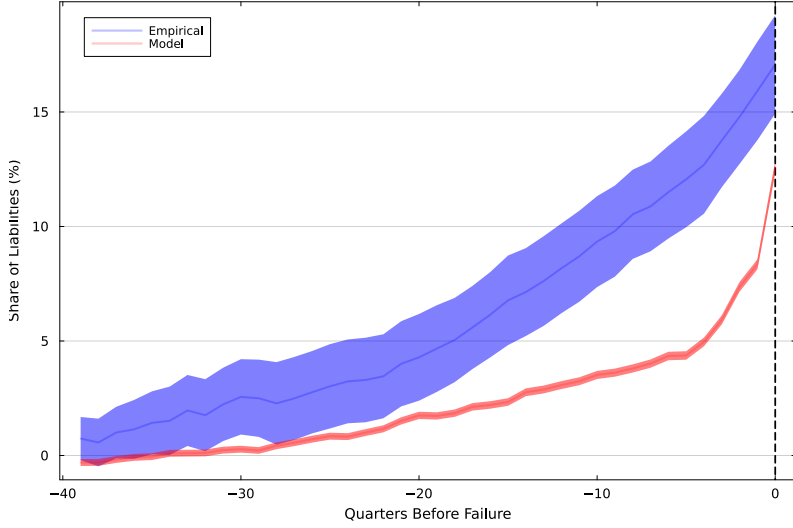


Figure 6: Time Deposits as a Share of Total Liabilities Before Bank Failure

Profitability Dynamics. Figure 7 compares the evolution of the net interest margin (NIM) in the data and in the simulated model around episodes of bank failure. Both series display a pronounced and sudden decline in NIM beginning roughly ten quarters before default, reflecting a sharp compression of lending margins as funding costs rise and profitability deteriorates. The model closely replicates this nonlinear pattern, matching the timing and intensity of the drop observed in the data. This sharp contraction in margins highlights how, late in the distress cycle, rising deposit rates and greater reliance on costly time deposits erode banks' profitability, ultimately precipitating default.

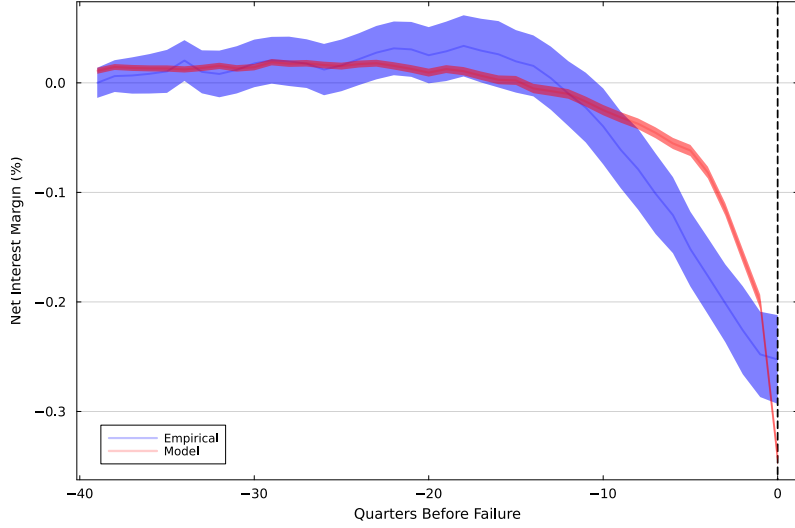


Figure 7: Net Interest Margin Before Bank Failure

Credit Losses. Figure 8 compares the evolution of net charge-offs in the data and in the simulated model around bank failures. Both series show a noticeable increase in charge-offs beginning roughly fifteen quarters before default, indicating a progressive deterioration in loan performance as banks approach distress. The model successfully reproduces the timing and trajectory of this increase, though it understates the final magnitude of losses observed in the data. This pattern reflects the buildup of credit risk that accompanies the funding and profitability pressures documented above: as margins compress and leverage rises, weaker balance sheets amplify exposure to loan defaults, eventually triggering bank failure.

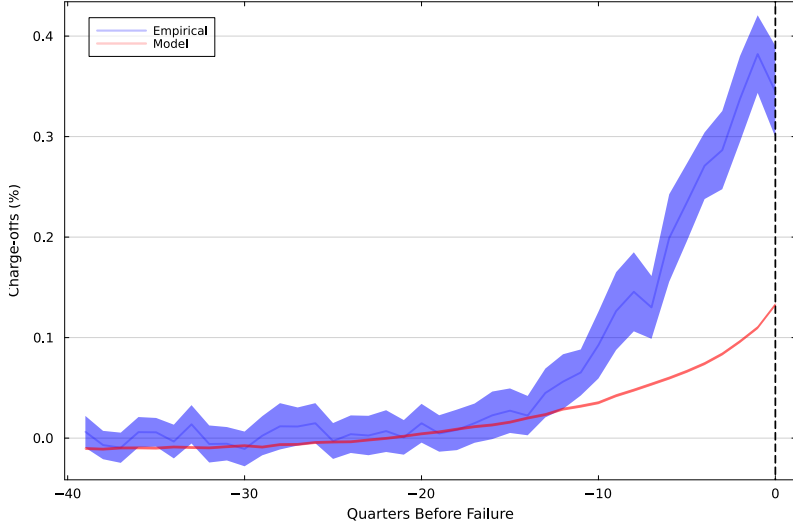


Figure 8: Net Charge-Offs Before Bank Failure

Taken together, these untargeted moments show that the model successfully reproduces the sequence of deterioration that precedes bank failure. It captures the gradual buildup of leverage, the shift toward illiquid and costly funding, and the sharp compression in profitability that ultimately culminate in rising loan losses and default. Although the model understates the final magnitude of charge-offs, it closely matches the timing and co-movement of key variables observed in the data. Overall, these results indicate that the mechanisms governing funding, risk-taking, and solvency in the model provide a coherent quantitative account of the dynamics of financial distress in the banking sector.

Breaking Down the Mechanism

To understand how the model replicates the empirical patterns, I examine how the optimal policy functions interact with the bank's value function with respect to its liquidity position n and its outstanding stock of time deposits b . This decomposition illustrates how balance-sheet decisions respond to liquidity, rollover risk, and the maturity structure of liabilities.

Figure 9 plots the optimal choice of time deposits as a share of total liabilities across the state space. The policy is monotone in the two state variables: the time-deposit share is increasing in the inherited stock of time deposits b and decreasing in cash-on-hand n . The bright band in the upper-left region corresponds to states with low liquidity and large outstanding time

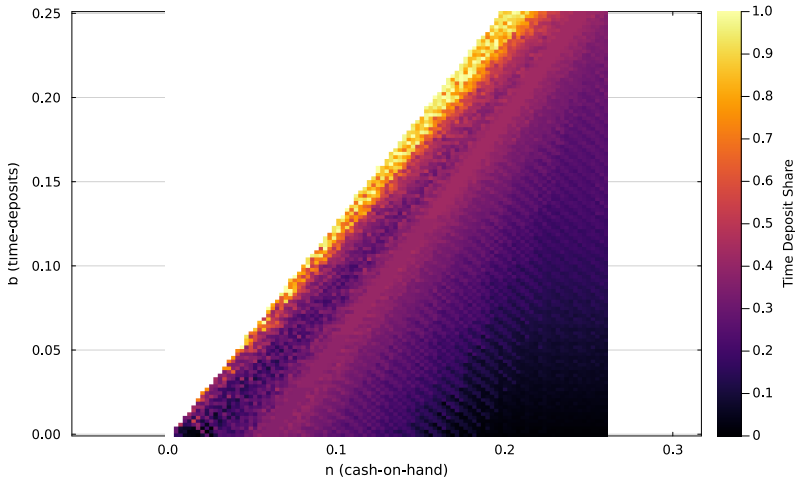


Figure 9: Optimal share of time deposits across the state space at best z

deposits—states close to default. In these distressed situations, banks optimally tilt their funding mix toward long-maturity liabilities, choosing time-deposit shares near one to lock in funding and reduce immediate rollover pressure.

As we move toward states with higher cash-on-hand or lower outstanding time deposits, the optimal time-deposit share declines smoothly. Banks that are far from default rely more heavily on short-term deposits, valuing the flexibility of short-maturity funding over the insurance provided by long-term liabilities. This pattern shows that the model concentrates long-maturity funding precisely where rollover risk is most severe.

To further understand why these patterns arise, Figure 10 plots the optimal dividend payout. Dividend payments are sharply state-dependent and display a clear threshold structure. Banks near the default region—characterized by low liquidity n relative to outstanding time deposits b —pay zero dividends, as preserving internal liquidity is more valuable than distributing resources to shareholders. This dark diagonal region aligns with the frontier where the bank is most at risk of violating its funding constraint.

Moving away from this boundary, dividend payouts increase smoothly. Banks with sufficient cash-on-hand relative to their time-deposit burden begin paying positive dividends, and the payout rises rapidly in states where liquidity is abundant. The bright region in the lower-

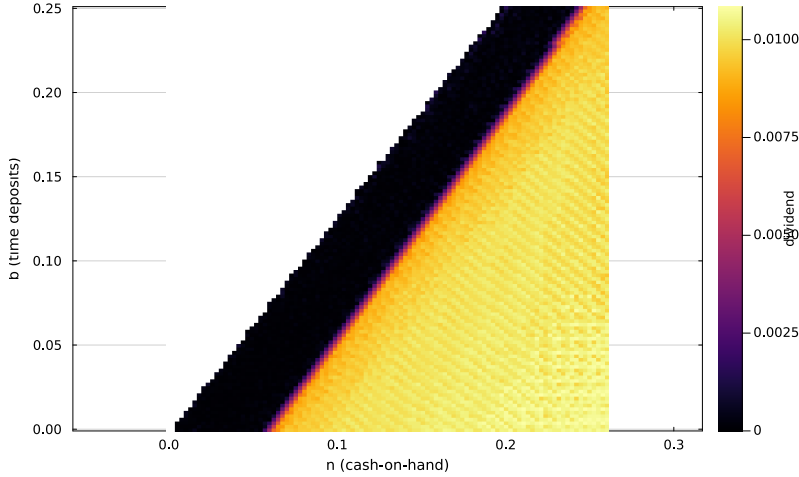


Figure 10: Optimal dividend payout across the state space at best z

right portion of the figure corresponds to banks that face minimal rollover risk. For these banks, the marginal value of internal funds is low, making dividend distribution the optimal use of excess resources.

Taken together, the dividend and time-deposit policies trace out a coherent mechanism: near-default banks hoard liquidity and extend the maturity of their liabilities, while well-capitalized banks relax both margins—reducing long-term funding and distributing dividends more aggressively.

Lastly, to understand the mechanism behind the relaxation channel of time deposits, I examine how marginal changes in liquidity and outstanding time deposits affect the bank’s continuation value. Specifically, I plot the derivatives of the value function with respect to n and b . These objects capture how valuable an additional unit of internal liquidity is, and how costly an additional unit of outstanding long-maturity liabilities becomes, across the state space. Comparing $\partial V/\partial n$ and $\partial V/\partial b$ reveals why distressed banks hoard liquidity and increase their reliance on time deposits, while well-capitalized banks relax both margins.

Figure 11 displays these derivatives at the highest productivity state z . The panels reveal a sharp asymmetry in how banks value liquidity versus long-term liabilities.

Panel (a) shows that $\partial V/\partial n$ is extremely high along the default frontier, where cash-on-hand

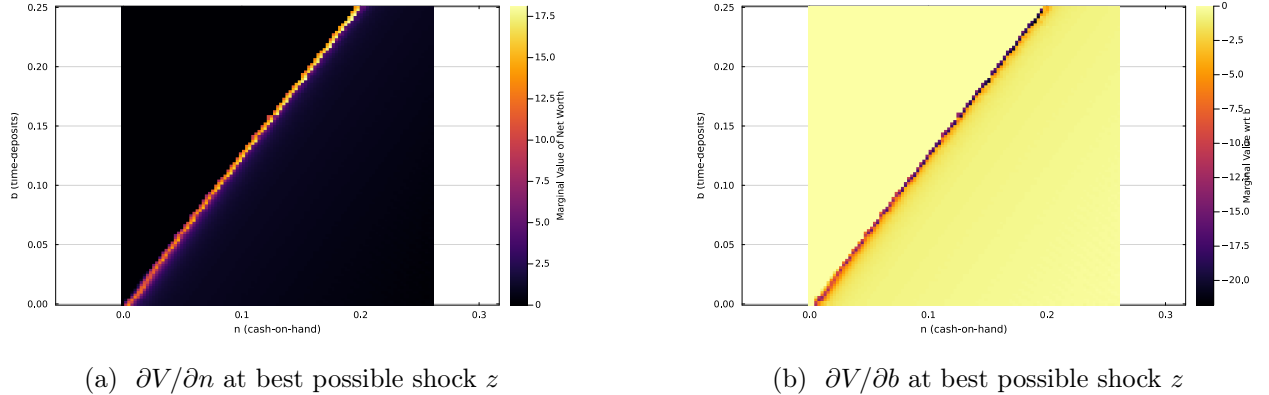


Figure 11: Derivatives of the value function with respect to liquidity and time deposits

is low relative to outstanding time deposits. In this distressed region, an additional unit of liquidity generates a steep increase in continuation value, reflecting the bank's urgent need to meet funding obligations and avoid insolvency. As n increases, the marginal value of liquidity declines rapidly, approaching zero for well-capitalized banks that are far from violating their funding constraint.

Panel (b) displays the opposite pattern for $\partial V / \partial b$. Near the default frontier, the marginal cost of additional time deposits is strongly negative: issuing more long-term liabilities sharply reduces continuation value because it tightens the funding constraint and raises rollover pressure in subsequent periods. As liquidity rises, the marginal cost of time deposits becomes small in magnitude—approaching zero for banks with substantial cash buffers. In these regions, long-maturity liabilities are almost neutral for continuation value, as rollover risk is negligible.

Taken together, these derivatives provide the key intuition for the model's mechanism. Distressed banks face a high marginal value of liquidity and a high marginal cost of additional long-term liabilities. As a result, they optimally hoard liquidity and tilt toward time deposits to relax future rollover pressure. Conversely, well-capitalized banks experience nearly flat marginal values along both dimensions, enabling them to reduce time-deposit issuance and distribute dividends more aggressively. These gradients in the value function are precisely what generate the monotone policy patterns shown earlier.

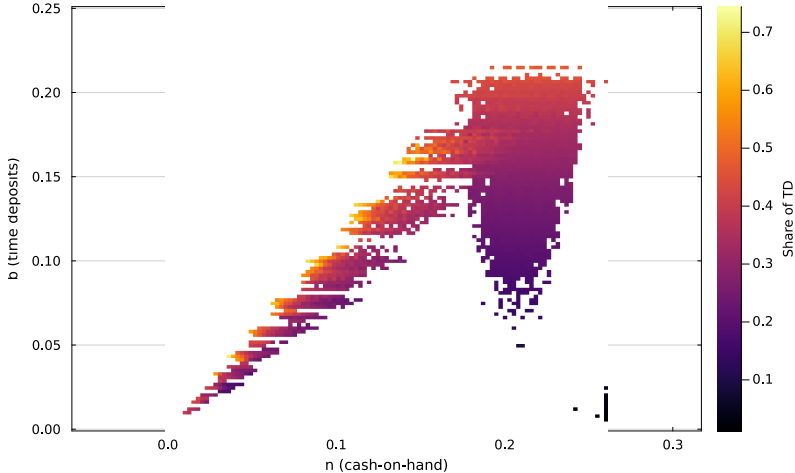


Figure 12: Inherited share of time deposits across the state space

To conclude, Figure 12 plots the inherited share of time deposits for the empirically relevant region of the state space, showing the combinations of (n, b) where the stationary distribution assigns significant probability mass. Two features stand out. First, banks rarely operate in the distressed portion of the state space where the optimal policy implies time-deposit shares close to one; these high-time-deposit states lie close to the default frontier and are visited infrequently in equilibrium. Second, most banks cluster in a region with intermediate shares of time deposits, where liquidity is sufficient to avoid rollover pressure but not so abundant as to make long-maturity funding redundant. This distributional pattern confirms the mechanism: the model endogenously pushes banks away from the extreme corner associated with rollover stress, resulting in a realistic mix of short- and long-maturity liabilities in steady state.

Breaking Down the Roles of the Model Parameters

To understand how the model generates the observed policy functions and the buildup of fragility, it is useful to unpack how the key structural parameters shape the bank's continuation value and the tightness of its constraints. In particular, the behavior of the marginal value of liquidity, $\partial V/\partial n$, provides a transparent lens into the mechanisms that discipline funding choices, rollover exposure, and default risk. Several parameters affect this object

through different channels. Below, I describe the role of each parameter that materially influences the slope of the value function and, consequently, the bank’s optimal policies.

Volatility of the Liquidity Shock (η_ω). The steep increase in $\partial V/\partial n$ near the default region is governed primarily by the parameter η_ω , which controls the volatility of the liquidity shock. A larger η_ω raises the probability that—even from moderate levels of liquidity today—the bank is pushed into a low- n state tomorrow where the funding and capital constraints bind. Since these low-liquidity states carry high default risk, the marginal value of liquidity rises sharply as the bank approaches the default boundary. Thus, η_ω determines how quickly $\partial V/\partial n$ becomes steep in the vicinity of default by expanding the set of states in which liquidity shortages are likely to occur.

Operating Cost (ψ). The fixed operating cost increases the amount of internal liquidity the bank must generate each period to remain solvent. A higher ψ raises the value of retaining earnings rather than expanding the balance sheet through external liabilities. As a result, banks place greater weight on preserving internal liquidity, shifting away from reliance on costly funding—especially time deposits—and toward retaining earnings to absorb operating expenses. This increases the shadow value of liquidity in low- n states and steepens the curvature of the value function near the default region, as internal liquidity becomes essential for keeping the bank outside the constraint set.

Managerial Myopia (σ). Managerial myopia influences how much the banker values future continuation relative to current dividends. A lower σ effectively compresses the future payoff, making it costlier (in utility terms) to retain liquidity for survival rather than distributing dividends today. This weakens precautionary motives and flattens $\partial V/\partial n$ away from the default boundary. However, because myopic managers are more willing to gamble for survival, σ also affects how sharply the value function declines when entering the region where constraints bind. Thus, σ modifies the slope of the value function primarily through intertemporal trade-offs.

Capital Requirement (κ). The capital requirement directly shifts the location of the default boundary. A higher κ makes the constraint $e' \geq \kappa a'$ more binding, expanding the set of states in which low liquidity leads to insolvency and effectively shifting the default

threshold to the right, toward states with higher levels of liquidity. As a result, an increase in κ raises $\partial V/\partial n$ in the vicinity of the constraint, since additional liquidity more effectively relaxes the capital requirement. This mechanism operates through the regulatory wedge: stricter capitalization elevates the marginal value of internal liquidity as a buffer against default.

Debt Issuance Cost (ζ). The convex cost of raising short- and long-term liabilities affects how easily banks can substitute external funding for internal liquidity. A higher ζ increases the marginal cost of issuing deposits or time deposits, making liquidity shortages more severe. When ζ is high, banks rely more on internal liquidity to satisfy regulatory and funding constraints, which steepens $\partial V/\partial n$ across a broader region of the state space. Conversely, low issuance frictions flatten the value function by allowing banks to raise external funds cheaply.

Taken together, these parameters jointly shape the slope of the value function and the tightness of the bank’s constraints. Their interactions determine the pattern of policy functions, the location of the default region, and the buildup of fragility observed in both the data and the calibrated model.

Variance Decomposition of Default

To connect the model most directly to the predictability patterns documented by Correia et al. (2023), I begin with a restricted variance decomposition that mirrors the information set in their empirical analysis. In particular, I regress the expected default probability on the two funding variables available in their setting—the share of time deposits and leverage—and compute their contributions using a two-variable *Shapley-value* decomposition. With only two regressors, each variable’s contribution corresponds to the average of its marginal explanatory power when entering the prediction model first versus second, yielding an internally consistent and order-invariant allocation of the variance they jointly explain.

Figure 13 displays the resulting decomposition over the forty quarters preceding failure. Consistent with the evidence in Correia et al. (2023), both time deposits and leverage explain very little of the cross-sectional variation in expected default far from failure, reflecting the relative homogeneity of solvent banks. Their explanatory power rises significantly only as

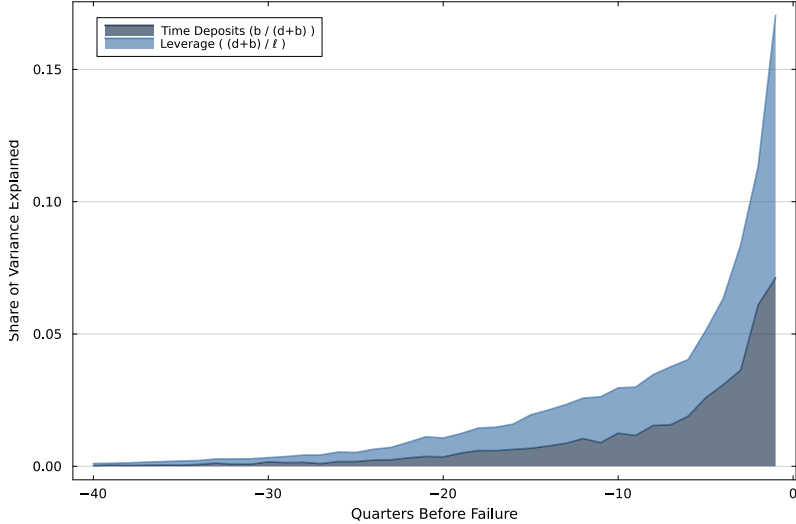


Figure 13: Restricted variance decomposition using leverage and time deposits.

failure approaches, indicating that funding structure becomes increasingly informative about distress as balance sheets deteriorate. Leverage captures the late-cycle surge in indebtedness, while the rise in time deposits reflects banks’ shift toward more illiquid funding as cash flow pressures mount.

Having established the model’s ability to replicate the empirical predictability patterns based solely on funding structure, I next turn to the full decomposition that includes loan losses. This richer specification regresses the expected default probability on the share of time deposits, leverage, and loan losses, and computes their contributions using the full Shapley-value approach. Each variable’s contribution is the average of its marginal explanatory power across all possible orders in which the three regressors can enter the model, ensuring an order-invariant breakdown of the total explained variance.

Figure 14 reports the full decomposition. Early in the event window, all components explain less than 1% of the cross-sectional variation in expected default, consistent with the uniform stability of solvent banks. As failure approaches, however, loan losses emerge as the dominant driver: their contribution rises sharply over the final twenty quarters and accounts for the majority of the variation in expected default at the point of collapse. Leverage contributes modestly and only near failure, while the share of time deposits plays a smaller but meaningful role in shaping the slow-moving buildup of fragility.

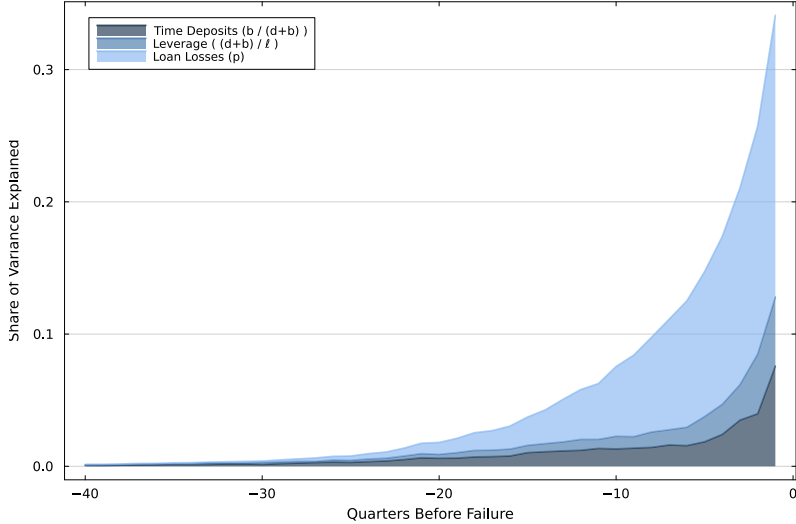


Figure 14: Full variance decomposition of expected default probability.

To further interpret these mechanisms through the lens of the model, Appendix C.2 presents an analogous decomposition based on the deeper structural state variables—cash-on-hand n and the liquidity shock ω —which clarifies how liquidity conditions feed into the buildup of fragility. Unsurprisingly, this liquidity-management margin emerges as the main driver of subsequent fragility, and it is strongly correlated with banks’ funding choices.

Taken together, the restricted and full decompositions provide a compelling picture: funding structure contains substantial predictive power for future bank distress, especially in the quarters immediately preceding collapse, while the sharp rise in expected default risk is ultimately driven by deteriorating asset quality. The model therefore captures both the slow-moving buildup of vulnerability from funding choices and the rapid acceleration in risk associated with worsening fundamentals.

Counterfactual – The Role of Time Deposits

To understand the mechanism behind these dynamics, I consider a counterfactual economy in which banks cannot issue time deposits. In this general equilibrium experiment, banks must rely entirely on short-term deposit funding, and all prices and aggregates adjust endogenously. Comparing this counterfactual with the benchmark economy shows how access to time deposits relaxes funding constraints, affects the cost of liquidity, and influences bank

failures.

General Equilibrium. Table 5 summarizes the general equilibrium differences between the benchmark model and the counterfactual economy without time deposits. Removing the option to issue time deposits leads to a minimal decline in the share of failing banks—from 0.084 percent to 0.083 percent—although banks deleverage and operate more conservatively. Average leverage falls from 87.34 percent to 84.31 percent, with higher dispersion, reflecting greater heterogeneity in balance-sheet adjustments as institutions manage rollover risk without access to illiquid funding. In turn, the net interest margin (NIM) rises from 1.00 to 1.16 percent, as the absence of costly time deposits lowers average funding costs and increases the spread between lending and deposit rates. Despite these higher margins, overall lending contracts slightly, from 12.30 to 12.03, as banks reduce balance-sheet size to mitigate liquidity risk, which represent a decrease of 2.15% in aggregate lending/capital. Together, these results illustrate the key general equilibrium trade-off: while the removal of time deposits reduces average default rates and raises profitability in the short run, it compresses credit supply.

Table 5: Targeted Moments: Benchmark Model, and Counterfactual

Moment	Benchmark (%)	Counterfactual (%)
Share of failing banks	0.084	0.083
Leverage	87.34	84.31
Share of time deposits	35.05 (11.59)	—
Net interest margin	1.03	1.16
Spread btwn. time dep. and deposit	0.34	—
Lending	12.30	12.03

Note: Standard deviations are shown in parentheses. Model and counterfactual moments correspond to the stationary equilibria of the benchmark and no-time-deposit economies, respectively. Lending values are reported in model units (not percentages).

Leverage Dynamics. Figure 15 compares the evolution of leverage ratios in the data and in the simulated model around episodes of bank failure, when time deposits are no longer available. Unlike in the benchmark economy, where leverage rises gradually as banks rely on illiquid liabilities to smooth funding shocks, in this counterfactual the absence of time deposits amplifies rollover risk. Without access to long-term funding, banks are forced to rely exclusively on short-term deposits, making them more vulnerable to liquidity shocks,

as captured by ω_t . As a result, they actively deleverage in anticipation of rollover risk, leading to a steady decline in leverage well before default. This pattern highlights that time deposits play a critical stabilizing role in the benchmark economy: by reducing debt repayment pressure, they mitigate rollover risk and allow banks to sustain higher leverage levels without immediate default.

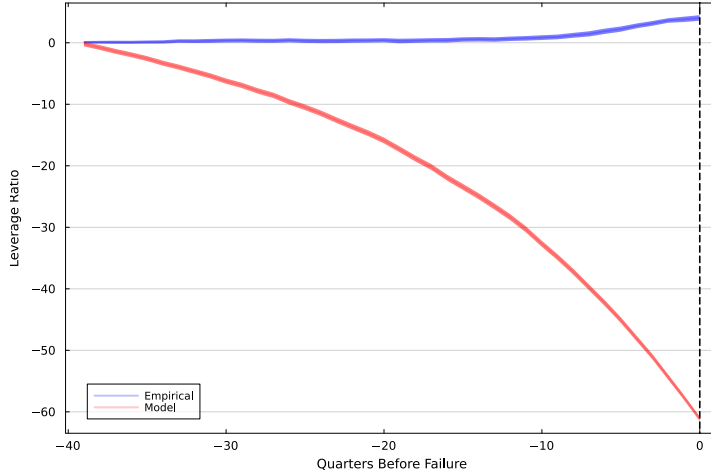


Figure 15: Leverage (Total Liabilities/Total Assets) Before Bank Failure Counterfactual

Profitability Dynamics. Figure 16 compares the evolution of the net interest margin (NIM) in the counterfactual economy without time deposits to the empirical pattern observed among failing banks. In the data (blue), NIM remains relatively stable for many quarters prior to failure, declining only gradually as conditions worsen. In the counterfactual model (red), however, profitability deteriorates immediately and declines steadily as the bank approaches default.

Without access to long-maturity time deposits, funding costs become increasingly sensitive to liquidity stress. As rollover risk intensifies and the bank relies exclusively on short-term deposits, deposit rates rise and lending spreads compress. This leads to a persistent and accelerating decline in NIM throughout the pre-failure window. The sharp collapse in NIM immediately before default reflects the bank’s inability to smooth funding pressures or maintain stable margins in the absence of illiquid long-term liabilities.

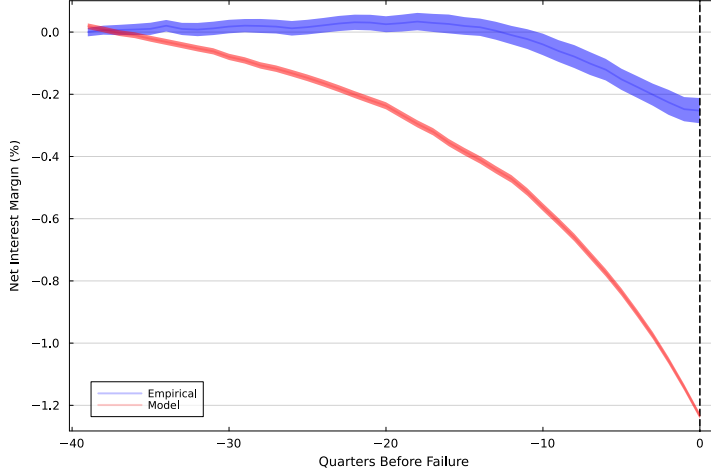


Figure 16: Net Interest Margin Before Bank Failure Counterfactual

Credit Losses. Figure 17 compares the evolution of net charge-offs in the counterfactual economy—where time deposits are unavailable—to the empirical pattern. The dynamics of credit losses remain broadly consistent across both settings: charge-offs begin to rise roughly thirty quarters before default, signaling a gradual deterioration in loan performance as banks approach distress, though the onset occurs earlier than in the benchmark model. In the absence of time deposits, however, the increase in charge-offs is somewhat more muted, as banks deleverage sooner and maintain smaller balance sheets. This close correspondence in dynamics, despite differences in leverage and profitability, highlights that deteriorating asset quality is a robust precursor to failure, largely driven by worsening borrower fundamentals rather than by the specific composition of bank funding.

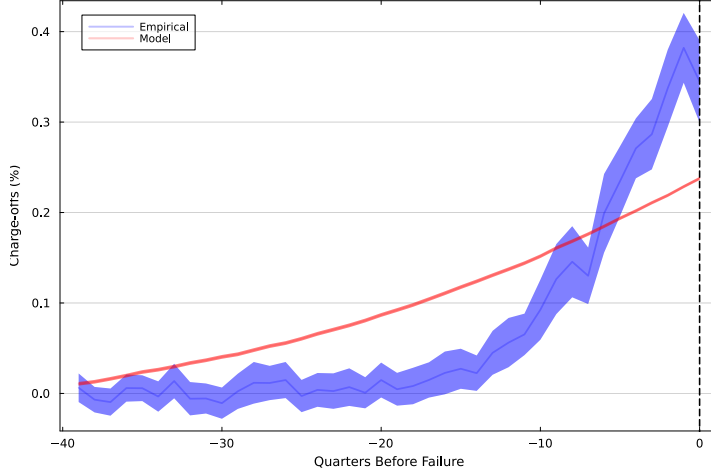


Figure 17: Net Charge-Offs Before Bank Failure Counterfactual

To understand why the counterfactual without time deposits behaves so differently, Figure 18 compares the derivative of the value function with respect to liquidity n in the two models, excluding the zero-liquidity point which corresponds to default. Across all economically relevant levels of n , the marginal value of liquidity is strictly higher in the deposit-only model (solid blue). Without access to long-maturity liabilities, banks rely entirely on short-term deposits, making their continuation value much more sensitive to fluctuations in internal liquidity. Even moderate reductions in n sharply increase the likelihood of hitting the constraint, so $\partial V / \partial n$ remains elevated throughout the low- and mid-liquidity region.

By contrast, when time deposits are available (dashed orange), the marginal value of liquidity is uniformly lower. Long-maturity liabilities reduce rollover pressure and relax the funding constraint, so additional liquidity contributes less to the bank's continuation value. Time deposits therefore flatten the liquidity wedge, making banks less fragile to small movements in n and weakening the incentive to engage in defensive deleveraging when liquidity falls.

Taken together, these counterfactual results highlight the central role of time deposits in stabilizing banks' balance sheets and mitigating liquidity risk. When banks lose access to this form of illiquid funding, their exposure to rollover risk increases sharply, prompting earlier deleveraging and a contraction in balance-sheet size. Although profitability initially improves because core deposit rates are less sensitive to default risk, this gain is short-lived: the absence of stable funding amplifies vulnerability to liquidity shocks and accelerates

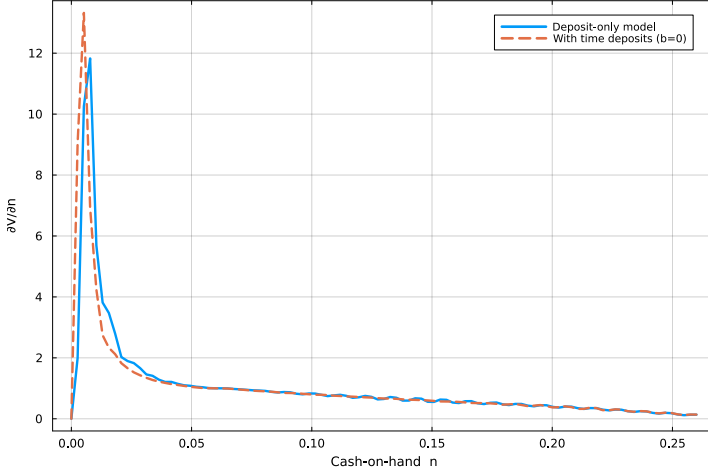


Figure 18: Derivative of the Value Function with Respect to n

default. In general equilibrium, time deposits therefore act as a crucial buffer that enables banks to sustain higher leverage and smoother funding conditions, ultimately reducing the frequency and severity of balance-sheet crises.

The Effects of Capital Regulation

Table 6 reports the steady-state moments for the benchmark economy and for a version of the model with a higher Tier 1 capital requirement of 8 percent.

Increasing regulatory capital reduces banks' failure risk. The quarterly share of failing banks declines from 0.084 percent in the benchmark to 0.066 percent under the high-capital regime. Although this difference is small in any given quarter, it compounds substantially over time. Over a 25-year horizon (100 quarters), the implied cumulative failure probability falls from roughly 8.4 percent to 6.6 percent, a reduction of about 1.8 percentage points. Importantly, this improvement in stability occurs without a meaningful change in average leverage, which decreases only slightly from 87.34 percent to 86.99 percent. Banks already maintain internal capital buffers in response to underlying credit and liquidity risk, so the higher regulatory minimum does not force a substantial deleveraging.

The tighter requirement also shifts banks' funding choices. The average share of time deposits declines from 35.05 percent in the benchmark to 33.17 percent under higher capital requirements. In the model, banks use time deposits as a precautionary source of more

stable, illiquid funding when rollover risk is elevated. Improved capitalization reduces the likelihood of entering the distress region, thereby lowering the incentive to rely on such precautionary funding. Consistent with this adjustment, the spread between time-deposit rates and regular deposit rates narrows (from 0.34 percent to 0.25 percent), while the net interest margin increases modestly (from 1.03 percent to 1.05 percent).

The aggregate implications are modest. Lending falls slightly—from 12.30 to 12.28 model units—corresponding to a decline of about 0.16 percent. Banks hold somewhat more capital, as required, but the overall scale of their balance sheets remains nearly unchanged.

Table 6: Targeted Moments: Benchmark Model, and Higher Capital Requirement

Moment	Benchmark (%)	Higher Capital (%)
Share of failing banks	0.084	0.066
Leverage	87.34	86.99
Share of time deposits	35.05 (11.59)	33.17 (11.48)
Net interest margin	1.03	1.05
Spread btwn. time dep. and deposit	0.34	0.25
Lending	12.30	12.28

Note: Standard deviations are shown in parentheses. Model and higher capital moments correspond to the stationary equilibria of the benchmark and an economy with a capital requirement of 8%, respectively. Lending values are reported in model units (not percentages).

These muted effects are consistent with the variance-decomposition results from the previous section. The decomposition shows that most of the variation in expected default arises from movements in loan charge-offs, particularly in the quarters immediately preceding failure. Liquidity contributes somewhat during the mid-distress phase, while leverage and maturity choice explain only a significant share of the variation at the middle of the event window. Raising regulatory capital increases banks' distance from the default boundary, but because default risk in the model is ultimately driven by large credit losses—rather than by funding maturity or leverage dynamics—a moderate increase in required capital cannot fully offset the shocks that push banks into distress. As a result, higher capital reduces failure risk only gradually, even though it improves the overall resilience of bank balance sheets.

Overall, this counterfactual demonstrates that higher capital requirements primarily operate by strengthening banks' balance sheets and reducing their exposure to rollover risk, rather

than by significantly altering leverage or lending activity. The adjustments across moments are modest, indicating that a moderate increase in regulatory capital ratios can enhance stability with limited impact on aggregate intermediation.

A related counterfactual, presented in Appendix C.3, explores the same increase in the Tier 1 capital requirement in a version of the model without time deposits. This experiment delivers two additional insights. First, the reduction in failure risk is of a similar magnitude to the benchmark model, indicating that the stabilizing effect of higher capital does not rely on banks' ability to adjust the maturity composition of their funding. Second, average leverage increases rather than falls. This occurs because the banks most affected by the higher capital requirement are precisely those that, in the baseline economy, approach default and respond by aggressively deleveraging. By pushing these marginal banks farther from the default boundary, the regulation prevents this sharp deleveraging episode from taking place and keeps them operating with comparatively thinner capital buffers. As a result, their continued presence in the market mechanically raises average leverage among surviving banks. Finally, aggregate lending rises in this version of the model, since improved bank survival expands the supply of credit. Taken together, these results imply an unambiguous welfare improvement: the counterfactual model experiences fewer failures, more lending, and greater resilience, even though banks lack access to the precautionary liquidity margin present in the benchmark environment.

5. Conclusion

This paper develops and quantifies a model of bank failures that links funding frictions to the gradual buildup of fragility observed in U.S. commercial banks. Empirically, I show that banks approaching failure systematically reshape their funding structure: they rely more heavily on time deposits, face rising funding costs, and experience deteriorating profitability, leverage, and loan performance. These patterns suggest that liability composition is not merely a passive reflection of distress but an active margin through which banks attempt to manage rollover pressure and liquidity risk.

Motivated by these facts, I build a model in which heterogeneous banks choose between short- and long-maturity liabilities under limited commitment and capital regulation. Time deposits provide stable liquidity and help insulate banks from short-term refinancing risk,

but they also increase future repayment obligations and amplify balance-sheet fragility. The model generates endogenous default thresholds and reproduces the key empirical features of failure dynamics, including the slow rise in leverage, the shift toward illiquid funding, the compression in net interest margins, and the acceleration of charge-offs.

The counterfactual exercises highlight two central insights. First, removing access to time deposits forces banks to deleverage early and operate with smaller balance sheets to hedge rollover risk. This reduces failure rates but also compresses credit supply. Second, a moderate increase in Tier 1 capital requirements strengthens resilience primarily by lowering rollover risk rather than by restricting lending. Higher capital reduces the incentive to rely on time deposits, compresses funding spreads, and lowers cumulative failure probabilities over a multi-decade horizon, while leaving aggregate lending and leverage largely unchanged.

Together, these results show that the structure of bank funding and the strength of capital buffers jointly determine banks' vulnerability to shocks. Illiquid funding instruments, while costly, play a stabilizing role when liquidity conditions tighten, and well-designed capital requirements can reinforce this buffer without creating large distortions to credit supply. More broadly, the analysis provides an integrated framework linking banks' balance-sheet management, regulatory constraints, and default risk, offering a quantitative lens through which to evaluate policies aimed at reducing the social costs of bank failures.

References

- Amador, M. and Bianchi, J. (2024). Bank runs, fragility, and credit easing. *American Economic Review*, 114(7):2073–2110.
- Arellano, C., Bai, Y., and Kehoe, P. J. (2019). Financial frictions and fluctuations in volatility. *Journal of Political Economy*, 127(5):2049–2103.
- Begenau, J. and Landvoigt, T. (2022). Financial regulation in a quantitative model of the modern banking system. *The Review of Economic Studies*, 89(4):1748–1784.
- Bocola, L. and Dovis, A. (2019). Self-fulfilling debt crises: A quantitative analysis. *American Economic Review*, 109(12):4343–77.
- Chatterjee, S. and Eyigunor, B. (2012). Maturity, indebtedness, and default risk. *American Economic Review*, 102(6):2674–2699.
- Chen, Q., Goldstein, I., Huang, Z., and Vashishtha, R. (2024). Liquidity transformation and fragility in the us banking sector. *The Journal of Finance*, 79(6):3985–4036.
- Choudhary, M. A. and Limodio, N. (2022). Liquidity risk and long-term finance: Evidence from a natural experiment. *The Review of Economic Studies*, 89(3):1278–1313.
- Coimbra, N. and Rey, H. (2024). Financial cycles with heterogeneous intermediaries. *Review of Economic Studies*, 91(2):817–857.
- Corbae, D. and D’Erasco, P. (2021). Capital buffers in a quantitative model of banking industry dynamics. *Econometrica*, 89(6):2975–3023.
- Correia, S., Luck, S., and Verner, E. (2023). Failing banks. *Available at SSRN 4650834*.
- Crouzet, N. et al. (2016). Default, debt maturity, and investment dynamics. In *2016 Meeting Papers, Society for Economic Dynamics*, volume 533, pages 1635–1682.
- Diamond, D. W. and He, Z. (2014). A theory of debt maturity: the long and short of debt overhang. *The Journal of Finance*, 69(2):719–762.

- Geelen, T., Hajda, J., Morellec, E., and Winegar, A. (2024). Asset life, leverage, and debt maturity matching. *Journal of Financial Economics*, 154:103796.
- Gertler, M. and Kiyotaki, N. (2015). Banking, liquidity, and bank runs in an infinite horizon economy. *American Economic Review*, 105(7):2011–2043.
- Jiang, E. X. (2023). Financing Competitors: Shadow Banks’ Funding and Mortgage Market Competition. *The Review of Financial Studies*, 36(10):3861–3905.
- Lee, H., Lee, S., and Paluszynski, R. (2024). Capital regulation and shadow finance: a quantitative analysis. *Review of Economic Studies*, 91(5):3047–3084.
- Ottonello, P. and Winberry, T. (2020). Financial heterogeneity and the investment channel of monetary policy. *Econometrica*, 88(6):2473–2502.
- Tauchen, G. (1986). Finite state markov-chain approximations to univariate and vector autoregressions. *Economics letters*, 20(2):177–181.
- Vasicek, O. (2002). The distribution of loan portfolio value. *Risk*, 15(12):160–162.
- Wang, Y., Whited, T. M., Wu, Y., and Xiao, K. (2022). Bank market power and monetary policy transmission: Evidence from a structural estimation. *The Journal of Finance*, 77(4):2093–2141.
- Young, E. R. (2010). Solving the incomplete markets model with aggregate uncertainty using the krusell-smith algorithm and non-stochastic simulations. *Journal of Economic Dynamics and Control*, 34(1):36–41. Computational Suite of Models with Heterogeneous Agents: Incomplete Markets and Aggregate Uncertainty.

A. Empirical Appendix

A.1. Data Sources

Call Reports and Uniform Bank Performance Reports Data from the Call Reports are obtained from the Uniform Bank Performance Reports (UBPR), supplied by the FFIEC, covering the years 2001 to 2025. The Call Reports include all FDIC-insured commercial banks, savings banks, and savings associations. The dataset compiles quarterly reports from each insured institution and constructs standardized measures for a wide range of bank-specific ratios. All variable definitions follow the UBPR documentation.

All ratios are trimmed if they lie more than three standard deviations above the sample mean. Additionally, I winsorize all variables at the 2.5th and 97.5th percentiles.

Variable Definitions

Bank Leverage. Leverage is defined as the ratio of total liabilities (**RCON2948**) to total assets (**RCON2170**).

Net Interest Margin.

$$NIM_{j,t} = 100 \times \frac{RIAD4107_{j,t} - RIAD4073_{j,t}}{RCON3368_{j,t}}$$

where interest income (**RIAD4107**) and interest expense (**RIAD4073**) are expressed as quarterly flows and divided by the quarterly average of total assets (**RCON3368**).

Net Income Margin.

$$\text{Net Income Margin}_{j,t} = 100 \times \frac{RIAD4340_{j,t}}{RCON3368_{j,t}}$$

where net income (**RIAD4340**) is expressed as a quarterly flow and divided by the quarterly average of total assets (**RCON3368**).

Net Charge-offs.

$$nco_{j,t} = 100 \times \frac{RIAD4635_{j,t} - RIAD4605_{j,t}}{RCON3360_{j,t} + RCON3484_{j,t}}$$

where charge-offs on loans and leases (**RIAD4635**) and recoveries (**RIAD4605**) are expressed as quarterly flows and divided by the quarterly average of loans and leases (**RCON3360** plus **RCON3484**).

Interest Rate on Savings And Checking Accounts. The Savings And Checking Accounts deposit interest rate $\text{IntSavCheck}_{j,t}$ is computed as:

$$\text{IntSavCheck}_{j,t} = 100 \times \frac{(RIAD4508_{j,t} + RIAD0093_{j,t})}{RCONB563_{j,t} + RCON3485_{j,t}},$$

where $RIAD4508$ $RIAD0093_{j,t}$ denotes the quarterly flow obtained by differencing year-to-date interest expenses within each bank-year. Thus, the numerator captures interest paid on savings and checking deposits, while the denominator reflects the contemporaneous stock of savings and checking deposits.

Interest Rate on Time Deposits. The variable TD rate $_{j,t}$ is constructed according to the FFIEC reporting change effective in 2018:

$$\text{TD rate}_{j,t} = 100 \times \begin{cases} \frac{RIADHK03_{j,t} + RIADHK04_{j,t}}{RCONHK16_{j,t} + RCONHK17_{j,t}}, & \text{if reporting date} > 2017-01-01, \\ \frac{RIADA517_{j,t} + RIADA518_{j,t}}{RCONA514_{j,t} + RCONA529_{j,t}}, & \text{otherwise.} \end{cases}$$

where every interest expense is expressed as quarterly flows.

Time Deposits Below and Above the Insurance Limit. The stocks of time deposits below and above the FDIC insurance limit are defined according to the FFIEC reporting

change effective in 2018:

$$\text{TD}_{j,t}^{\text{below}} = \begin{cases} \text{RCONHK16}_{j,t}, & \text{if reporting date} > 2017-01-01, \\ \text{RCONA529}_{j,t}, & \text{otherwise,} \end{cases}$$

$$\text{TD}_{j,t}^{\text{above}} = \begin{cases} \text{RCONHK17}_{j,t}, & \text{if reporting date} > 2017-01-01, \\ \text{RCONA514}_{j,t}, & \text{otherwise.} \end{cases}$$

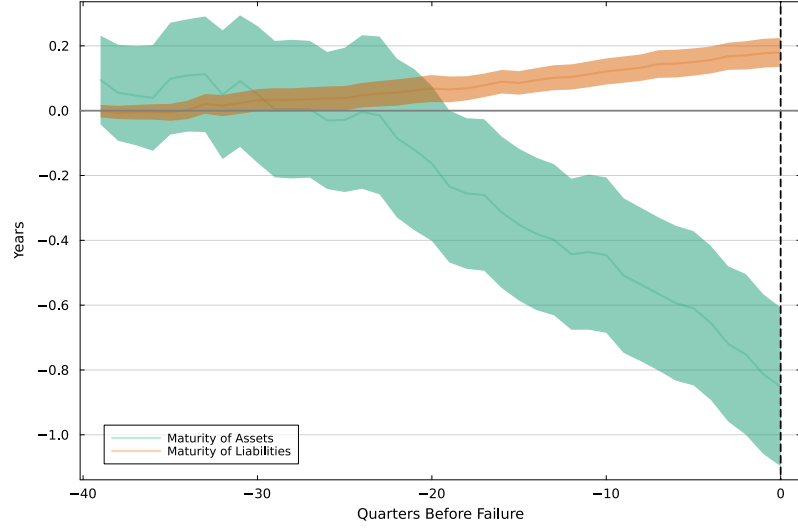


Figure A.1: Maturity of Assets and Liabilities Before Bank Failure

B. Model Appendix

Exit and Entry

Exit from the market is endogenous and depends on the bank's default decision. In each period, the mass of entering banks, μ_e , equals the mass of exiting banks. Each entrant is endowed with initial equity \bar{n} and begins operation with zero debt.

New banks inherit the pool of entrepreneurs previously served by exiting banks, thereby preserving the distribution of idiosyncratic shocks in the economy. This assumption captures the idea that entrants fill the market positions vacated by failed banks, maintaining a stable environment.

Monetary Authority

The final component of the model is the monetary authority, which determines the real interest rate.

Monetary Authority. The monetary authority sets the real risk-free rate $R_{f,t}$ according to:

$$\log(R_{f,t}) = -\log(\beta), \quad (\text{A.1})$$

implying a constant steady-state real rate consistent with the household's intertemporal discount factor.

Equilibrium

I now define the competitive equilibrium in the steady state.

Law of Motion for the Distribution of Banks. Before defining the equilibrium, I first characterize the evolution of the bank distribution in steady state, with an analogous structure during the transition.

Let the optimal policies conditional on states (z, n, b) be:

$$R_\ell^*(z, n, b), \quad d^{*\prime}(z, n, b), \quad b^{*\prime}(z, n, b),$$

where $R_\ell^*(z, n, b)$ is the optimal lending rate, $d^{*\prime}(z, n, b)$ the optimal deposit issuance, and $b^{*\prime}(z, n, b)$ the optimal long-term liability policy.

These policies may be empty when the non-negative dividend constraint is violated, in which case the bank defaults. Upon default, a new bank enters the economy with initial equity \bar{n} , no long-term liabilities, and inherits the exiting bank's client pool, characterized by the same p . In equilibrium, the mass of entrants equals the mass of defaulting banks, maintaining a constant measure of active banks over time.

Let μ denote the cross-sectional distribution of banks over (z, n, b) . The mass of exiting (defaulting) banks is given by:

$$\mu^e = \int h^*(z, n, b) d\mu(z, n, b),$$

where δ^* is the bank's default policy.

Define the law of motion for net worth as:

$$n'(z', \omega', p, n, b) = n'(z', \omega', R_\ell^*(z, n, b), d^{*\prime}(z, n, b), b^{*\prime}(z, n, b)),$$

and let the indicator function for next-period states be:

$$\mathbb{I}(z', \omega', n', b' | p, n, b) = \begin{cases} 1, & \text{if } (z', \omega', n', b') = (z', \omega', n'(z', \omega', p, n, b), b^*(z, n, b)), \\ 0, & \text{otherwise.} \end{cases}$$

The distribution of incumbent banks evolves according to:

$$\mu'_i(z', n', b') = \int (1 - \delta^*(z, n, b)) \mathbb{I}(z', \omega', n', b' | p, n, b) G(\omega') F(z' | z) d\mu(z, n, b),$$

where $G(\omega')$ and $F(z' | p)$ are the transition probabilities of the exogenous shocks ω and p , respectively.

Similarly, the distribution of entrant banks evolves as:

$$\mu'_e(z', n', b') = \int \delta^*(z, n, b) \mathbb{I}(z', \omega', n', b' | p, \bar{n}, 0) G(\omega') F(z' | p) d\mu(z, n, b).$$

Since entrants inherit the client pools of exiting banks, the entrant distribution depends on the same loan-performance state p .

The overall law of motion of the bank distribution is:

$$\mu'(z', n', b') = \mu'_i(z', n', b') + \mu'_e(z', n', b').$$

A stationary distribution satisfies:

$$\mu^*(z, n, b) = \mu'(z, n, b) = \mu(z, n, b),$$

implying that the inflow and outflow of banks are balanced, and the cross-sectional distribution of banks remains constant over time.

Capital Market Clearing. Consider the distribution of operating banks $\mu(z, n, b)$. Let $R_\ell^*(z, n, b)$ denote the optimal loan rate policy. Each bank's loan supply is given by $\ell^s(z, n, b) = \ell^d(R_\ell^*(z, n, b), R'_E)$.

Since banks may default, aggregate loan supply also accounts for new entrants:

$$L^s = \int [1 - \delta^*(z, n, b)] \ell^s(z, n, b) d\mu(z, n, b) + \int \delta^*(z, n, b) \ell^s(z, \bar{n}, 0) d\mu(z, n, b),$$

where the first term represents incumbent banks and the second represents entrants. Given the normalization of the capital price to one, market clearing in the capital market requires:

$$K' = L^s, \quad (\text{A.2})$$

where K' denotes aggregate capital next period.

Definition 1. A stationary competitive equilibrium consists of value functions $V(z, n, b)$; decision rules $R_\ell(z, n, b)$, $d'(z, n, b)$, $b'(z, n, b)$; a measure of banks $\mu(z, n, b)$; debt price schedules $q_d(z, R_\ell, d', b')$ and $q_b(z, R_\ell, d', b')$; a borrowing decision $\ell(R_\ell^j, R_E')$; and a set of prices P such that:

- Entrepreneurs maximize expected utility given the loan rate R_t^j , consistent with their borrowing decision and utility function;
- Banks choose $R_\ell(z, n, b)$, $d'(z, n, b)$, and $b'(z, n, b)$ to maximize their value functions;
- Households price default risk competitively and optimize their portfolio decisions;
- Firms maximize profits given factor prices;
- The distribution of banks $\mu(z, n, b)$ is consistent with individual policy functions and the law of motion above;
- All markets clear.

One of the key state variables of interest is the cross-sectional distribution of banks across (z, n, b) .

C. Quantitative Appendix

C.1. Algorithm for Steady State

The bank problem is solved using value function iteration (VFI) due to the existence of two defaultable liabilities, which might cause indeterminacy. In the benchmark setup, I have

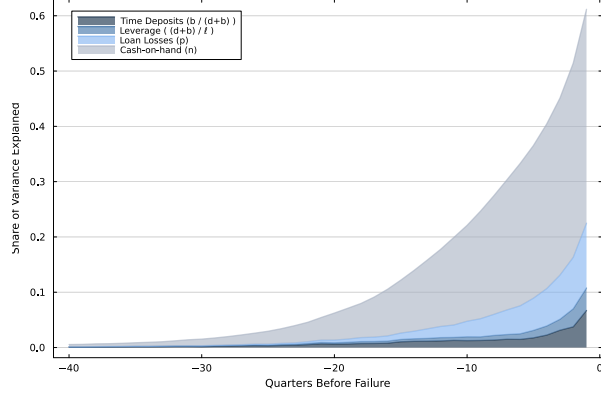


Figure C.1: Variance decomposition using leverage, time deposits, loan losses, and cash-on-hand

101, 201, and 121 grids for the endogenous choice variables, R_ℓ , d' , and b' , respectively. Additionally, I use 7 grid points for z , 101 for n , and 11 for ω . After each iteration, I update both liability prices to speed up the computational time, dampening the updates as the number of iterations increases. I stop the process if the distance between iterations is below a tolerance of 10^{-5} , due to the numerical precision of using single precision at the GPU. Then, I store the policies for each grid point of (z, n, b) .

The algorithm to solve the steady-state mass of banks according to their variables (z, n, b) follows Young (2010). Since the number of grid points for the endogenous variables for the cash-on-hand (n) is significantly smaller than the number of grid points for R_ℓ , d' , it generates a faster convergence speed than if I were to have (z, ℓ, d, b, ω) as state variables. Therefore, my vector for the steady state distribution is given by (z, n, b) , which has more than 70 thousand grid points. Finally, I compute a transition matrix for (z, n, b) , iterating with an initial guess for μ 5.000 times, which guarantees a convergence of the distribution.

C.2. Variance Decomposition

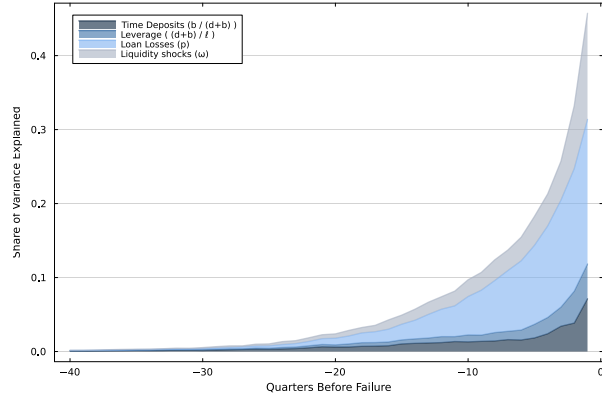


Figure C.2: Variance decomposition using leverage, time deposits, loan losses, and omega

C.3. Capital Regulation Without Time Deposits

Table 7: Targeted Moments: Counterfactual Model, and Higher Capital Requirement

Moment	Counterfactual (%)	Higher Capital (%)
Share of failing banks	0.083	0.069
Leverage	84.32	87.06
Net interest margin	1.16	1.18
Lending	12.04	12.09

Note: Standard deviations are shown in parentheses. Counterfactual model moments correspond to the stationary equilibria of the counterfactual model without time deposits and the same economy with a capital requirement of 8%, respectively. Lending values are reported in model units (not percentages).